ABSTRACT

GOTHI KULDIP SHUKDEVBHAI. Investigation of interconnect characteristics in mixed signal circuits. (Under the direction of Dr. Michael B. Steer)

Up to the early 1990s on chip digital signals had components much below 1 GHz, relatively short run lengths and widths of several microns. This situation has changed because of three main developments, primarily for digital circuits, but affecting analog circuitry because of the rise of mixed signal systems. The main developments are faster clocks, longer interconnect and fine lithography leading to interconnects having cross sectional dimensions of less than a micron. Planar structures such as microstrip lines are assuming very important role in the design of MICs and mixed signal circuits. Various design formulas for microstrip lines are investigated in this thesis. These formulas can be evaluated quickly and provide a designer with an intuitive feel for the various design parameters for microstrip lines. Various analytical formulas for microstrip dispersion are also compared with simulated results. Electromagnetic modeling tool from Sonnet® is used for high frequency electromagnetic analysis.

INVESTIGATION OF INTERCONNECT CHARACTERISTICS IN MIXED SIGNAL CIRCUITS

By

GOTHI KULDIP SHUKDEVBHAI

A thesis submitted to the Graduate Faculty of
North Carolina State University
in partial fulfillment of the
requirements for the Degree of
Master of Science

Electrical Engineering

Raleigh

May 2003

APPROVED BY:

_____ _____

_____
Chair of advisory committee

DEDICATION

I dedicate my thesis to my parents for providing me the motivation and support in my endeavors.

BIOGRAPHY

Gothi Kuldip S. was born in Ahmedabad, India in 1980. He completed his schooling at A. G. High School in May 1997. He got his Bachelors in Electronics & Telecommunications from L. D. College of Engineering (Gujarat University), Ahmedabad. As part of his final year curriculum project he worked at the Physical Research Laboratory, India's leading Scientific Research Institute. He came to North Carolina State University in fall 2001 for the Master of Science program in Electrical Engineering. During his stay at NC State he had a chance to work as an intern at MTS Systems Corporation-Sensors Division, NC.

ACKNOWLEDGEMENTS

I would like to express my gratitude to my advisor Dr. Michael B. Steer for his support and guidance in completing my Master's here at NC State University. I am really glad that I got the opportunity to work with him. I am really grateful to him for guiding me in the right direction. I am also grateful to my parents for guiding me in the right direction throughout my career.

I would also like to thank Dr. Griff Bilbro & Dr. Gianluca Lazzi for serving on my advisory committee and for their valuable suggestions.

Table of Contents

List of Figures

List of Tables

Chapter 1

Introduction

1.1 Background

Interconnects have achieved a prominent position in determining the performance of high-speed digital, RF and microwave circuits. In digital circuits, interconnect delay exceeds that of individual gates and is the primary determinant of clock speed. In RF and microwave circuits, interconnects and passive elements defined using them are critical circuit components.

Interconnect delay has become an important factor in the performance and design of high–speed interconnects in digital circuits. The key determinant of whether an interconnect can be considered as an invisible connection is whether the signal anywhere along the interconnect has the same value at a particular instant. If the value of the signal varies along the line, then it may be necessary to consider transmission line effects. In today's high clocking speed circuits, and at RF and microwave frequencies, retardation can be significant and an interconnect cannot be considered to be an instantaneous circuit, and transmission line structures are assuming more and more importance in high speed and mixed signal circuit design. In this thesis various design curves are developed that provide the circuit designer an intuitive feel for the important design parameters of microstrip circuits. The theoretical microstrip dispersion formulas are compared to the simulation results obtained by Sonnet Lite®.

1.2 Thesis Overview

The thesis is organized into six chapters. Chapter 1 introduces the necessary background and motivation behind this research.

Chapter 2 is a brief description of on chip interconnects for digital systems. Chapter 3 first describes various transmission line structures and then discussed fundamentals and various properties of microstrip line and dispersion effect in detail. Chapter 4 discusses how Sonnet Lite® operates and what the capabilities and applications of Sonnet Lite® are. Chapter 5 first describes the procedure for drawing geometry in Sonnet Lite®, then the simulation results obtained from Sonnet Lite® for various microstrip design formulas and dispersion formulas are plotted with the help of Microsoft Excel.

Chapter 2

On-Chip Interconnects for Digital Systems

2.1 Overview of on chip interconnects

Up to the early 1990's on chip digital signals had components much below 1 GHz which resulted in the electrical lengths of on-chip interconnects being much less than a wavelength of the signals present. Shrinking process technologies and increasing design sizes have continually challenge design methodologies. Before the complexities of deep submicron (DSM), gate and transistor delays dominated interconnect delays, and enabled simplified design methodologies that could focus on device analysis. The advent of DSM processes is changing all of this, invalidating assumptions and approximations that existing design methodologies are based upon.

As process technologies shrink, five different major effects occur:

- Device (gate) delays decrease, due to the thinning gate oxide
- Interconnect resistance increases, because of shrinking wire widths
- Vertical heights of interconnect layers increase, in an attempt to offset increasing interconnect resistance
- The area component of interconnect capacitance no longer dominates. Lateral (sidewall) and fringing components of capacitance start to dominate the total capacitance of the interconnect
- Interconnect capacitance dominates total gate loading

These changes directly affect the performance of a design and indirectly force a change in design methodology. The total delay associated with a net or path is governed by a simple equation that includes device delays, device loads, and slew rates. The delays caused by device loading are known as interconnect delays with the total delay represented as:

Total delay = device delay + interconnect delay + slew rate (see Figure 2.1)

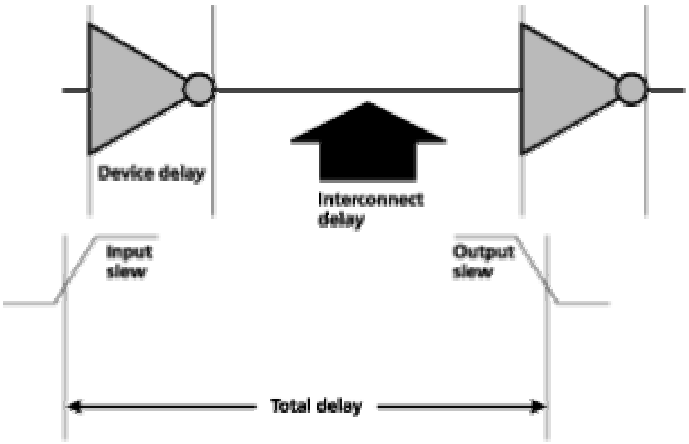

Figure 2.1: Total delay is equal to device delay plus interconnect delay and slew rate. Taken from [16].

When process geometries were greater than several microns, the performance of a design could be accurately predicted by analyzing device delays and approximating (or in some cases, ignoring) the interconnect delays and slew rates. Device loads were typically treated as a lumped capacitance, an approximation enabled by the fact that device delays dominated the equation. Slew rates were also typically ignored for the same reason.

As processes shrank below one micron and the faster clocks of gigahertz (and above) are used, these approximations became more and more inaccurate. With the total delay decreasing, slew could no longer be ignored, since it affected a more significant percentage of the total delay. For the same reason, device loads could no longer be accurately represented by lumped RC models.

2.2 Types of on chip interconnects

On chip interconnect have several distinguishing characteristics that can be used in determining the type of modeling required. An interconnect is not just a wire connecting one point in a circuit to another. There is always a current return path whether provided explicitly or not. The proximity of the return path to the signal path is equally important in determining the electrical characteristics of the interconnect. It contributes to the inductance, capacitance and resistance experienced by the signal. Without a return path charges would build up at some point in the circuit to very high levels, also the electric field supported by the charges on the signal conductor of an interconnect must terminate on matching charges, and these are located on the signal return path. Thus the signal return path plays a very important role in high speed circuit design

On chip interconnects can be broadly classified by the type of signals conveyed and geometrical and circuit characteristics as described below:

- Local interconnects with maximum length of 1–3 mm.

The majority of the connections on chip are of this type. Minimum line widths are used as dictated by the technology and these are in 0.1 to 0.5 μm range. This is known as deep sub micron region. It is not economical to provide metal for individual signal return path.

- Medium length connections with minimum length of 1–3 mm.

The maximum usable length is determined by the characteristics of the technology and of the interconnect itself. Typically the maximum usable length is around 2–5 mm.

- Long connections up to a chip–edge in length.

Three families of interconnections that are in this category are data buses, clock signal and control lines. Data buses are often wide and can be about half the chip-edge in length. Control signals transmit signals that must be widely distributed. Clock signal must be widely distributed with integrity of the signal being paramount.

- Power and ground distribution buses.

These buses carry large switching currents that change at the clocking frequency. The pulsing current transmits a signal just as real as do voltage variations. With fast chips it is necessary to model and design these as high speed interconnections.

2.3 Summary

The provision of a structure for a definite current return path is the easiest architectural approach to relieving the **interconnect delay problem.** Typical structures that provide close and well–defined current return paths are the microstrip, coplanar wave guide (CPW) and differential line or coplanar strips (CPS). The provision of a defined current return path is not the only consideration. Modern ICs use high aspect ratio interconnects with heights that can be twice the minimum conductor width. Chapter 3 discusses microstrip and various planner interconnects.

Chapter 3

Interconnect Technologies

3.1 Overview

Signals on high speed interconnects on semiconductor chips (ICs for Integrated Circuits) and multi chip modules (MCMs) are now extending into gigabit signal rates, which means that transmission line design issues apply. The transmission line structures are thus widely used. They are broadband in frequency and are generally economical to produce since they are readily adaptable to Microwave (hybrid) Integrated Circuits (MICs), Multichip Modules (MCMs), single chip packages and monolithic integrated circuits at RF and microwave frequencies. Each transmission line structure has its advantages with respect to others. This chapter provides an overview of these transmission line structures but discusses various properties of Microstrip Line in detail.

3.2 Transmission Line Structures

Many planar transmission line structures have been conceived and variants are still frequently being developed. Each type of line structure has potential advantages for various applications. Following is the list of all the common structures:

- Image line
- Microstrip
- Finline
- Inverted Microstrip
- Slot line
- Trapped Inverted Microstrip
- Strip line
- Suspended Strip line

- Coplanar Waveguide
- Embedded Differential Line
- Differential Line or Coplanar Structure (CPS)

Each structure comprises a combination of metal and dielectric layer. In most cases the dielectric principally supports the metal pattern, acting as a substrate, and clearly influences the wave propagation. For circuit applications the characteristic impedances achievable with these various structures need to be known. Table 3.1 lists the range of characteristic impedance that may be expected. These values are the practically realizable values determined by what can be fabricated, given manufacturing tolerances and avoiding multimoding.

Table 3.1: Characteristic Impedance (Z_0) ranges for the various structures with a substrate permittivity of 10. Taken from Edwards and Steer [11].

Structure	Z_0
Microstrip	11–110
Inverted microstrip	11–130
Trapped inverted microstrip (TIM)	14–140
Suspended strip line	40–150
Coplanar wave guide (CPW)	40–110
Differential line, coplanar strips (CPS)	40–110
Slot line	35–250
Finline	10–400
image line	$\cong$ 26

3.3 Microstrip Line

The microstrip line, Figure 3.1(d), is a very simple geometric structure, which consists of a metallic strip on a dielectric slab, which in turn, is backed by a conducting ground plane. Because of this planar geometry, microstrip readily lends itself to fabrication. The electromagnetic fields involved in microstrip line are complex and requires quite elaborate mathematical treatment. This section describes the geometry of microstrip line, mode of propagation, static TEM parameters, various synthesis formulas and dispersion effects.

3.3.1 Geometry of Microstrip Line

A microstrip is a two-conductor transmission line that can be considered to have evolved conceptually from a two-wire line.

In Figure 3.1 the transformation from (a) to (b) is essentially a change in the shape of the conductors, whereas that from (b) to (c) involves placing a conducting sheet at the plane of symmetry. The final configuration (d) is obtained by inserting a thin dielectric slab between the two conductors. As a consequence of the last step, the dielectric medium of the transmission line becomes inhomogeneous. The general three-dimensional geometry with all the parameters is shown in Figure 3.2.

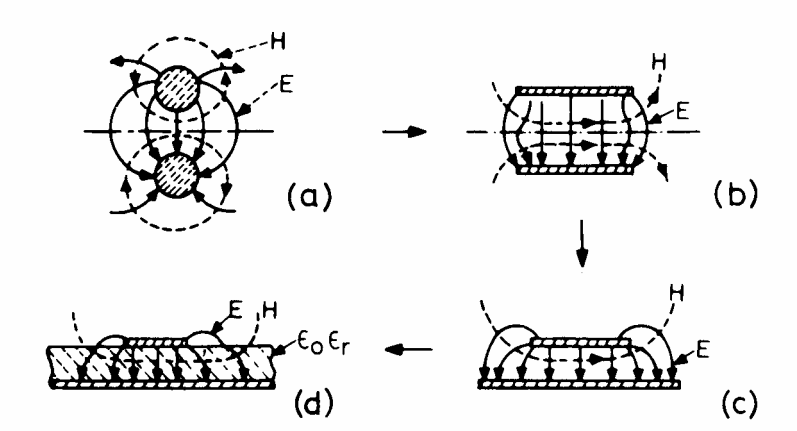

Figure 3.1: Conceptual evolution of a microstrip from a two-wire line.

Taken from Gupta [12].

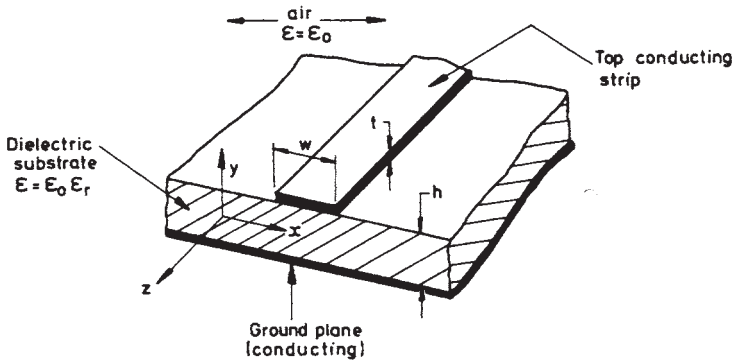

Figure 3.2: Three dimensional geometry of Microstrip line with all the parameters. Taken from Edwards and Steer [11].

Microstrip lines differ considerably from other transmission lines. For example, comparing it with a strip line, one observes that the microstrip structure is open at the top. This open configuration makes a microstrip very convenient for use in MICs where discrete lumped devices must be mounted in the circuit. Also small adjustments or tuning can possibly be incorporated after the circuit has been fabricated. However along with these advantages, the open structure of a microstrip causes some complications in microstrip analysis and design. This is due to the fact that the presence of the dielectric-air interface modifies the mode of propagation in a microstrip to a non-TEM hybrid mode (as compared to a pure TEM-mode in a strip line). The most important dimensional parameters are the microstrip width (w) and height (h). Also of great importance is the relative permittivity of the substrate, ε_r. In RF and microwave applications the thickness (t) of the metallic, top-conducting strip is generally of much lesser importance and may often be neglected. However, microstrip line in on-chip and on MCMs are relatively thick as a result of the need to keep resistance down while still achieving high wiring density by keeping width down.

3.3.2 Substrate Materials

The substrate is an integral part of the microstrip line and determines the electrical characteristics of the circuit. Together with the substrate thickness h, the permittivity

defines the basic operation of the structure. A good substrate material should have a uniform permittivity ε_r and thickness h over the whole structure, as well as for different batches of a given material, to ensure circuit reproducibility. The substrate material also provides mechanical support that ensures that implanted components are properly positioned and mechanically stable. The dielectric losses of the substrate should be small (ideally $\tan(\delta)$ < 0.001) in order to ensure high performance of circuits and acceptable quality factors for resonators filters, and radiating elements. Substrates can be grouped in five main categories: ceramic, synthetic, composite, semiconductor, and ferromagnetic. Some of the common materials on which microstrip circuits are fabricated are Alumina, RT/Duroid microwave laminates, Gallium Arsenide, and Sapphire. Table 3.2 lists dielectric constants for these materials. Sapphire has an anisotropic nature. It is crystalline and has different dielectric properties along different axes of the material. Gallium Arsenide is generally used for higher frequencies. Each material has advantages which make it desirable for some specific applications and disadvantageous which limit its usefulness in other applications. As a result, the first step to a successful design is a careful appraisal of the electrical and mechanical requirements. On this basis, the various material trade-offs can be evaluated and a choice made which is most appropriate for the specific application. There are further details on substrate materials in cited references [11] and [12].

Table 3.2: Dielectric constants of various materials.

Material	Dielectric Constant
Alumina	8 – 10
RT/duroid microwave laminates	2.23 – 2.33
GaAs	12.8
Sapphire	9.4/11.6

3.3.3 Mode of Propagation

Any transmission line that is filled with a uniform dielectric (i.e. homogeneous structure) can support at least one, well-defined mode of propagation, at least for a specified range of frequencies, provided that the geometries are not too large. It is clear from Figure 3.2 that the microstrip line involves an abrupt dielectric interface between the substrate and the air above it. The fields extend into two media, air above and dielectric below, so that the structure is inhomogeneous. Simple arguments based on the known quasi-static field distribution of the microstrip structure and Maxwell's equations can be presented to show that a microstrip structure cannot support a pure TEM wave. Over most of the operating frequency range of microstrips, the longitudinal components of the fields for the dominant mode remain very much smaller than the transverse components and may therefore be neglected. The dominant mode then behaves like a TEM mode and the bulk of energy transmitted resembles TEM, and thus it is usually referred to as the **quasi-TEM** approximation. The detailed field distribution is quite complicated, but the main transverse electric field can be visualized as shown in Figure 3.3. Representative views of the magnetic and electric field distributions are given in Figure 3.4.

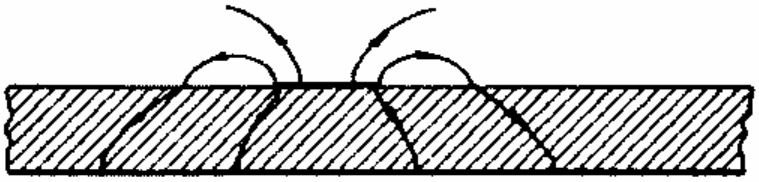

Figure 3.3: Transverse cross-section of microstrip, showing electric field. Taken from Edwards and Steer [11].

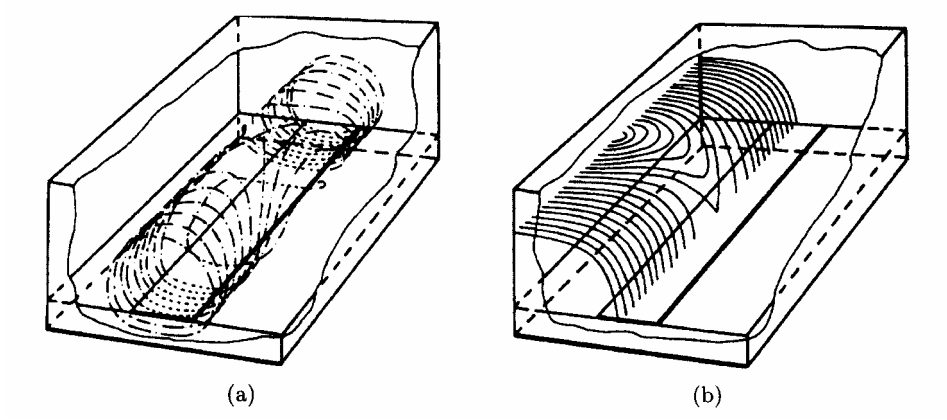

Figure 3.4: Three dimensional views of: (a) electric field; and (b) magnetic field. Taken from Edwards and Steer [11].

At most transverse cross-sectional planes, taken across the shielded microstrip, the electric (E) and magnetic (H) fields follow the distributions indicated in Figure 3.5. Note the abrupt change in the direction of the electric field line as it passes through the air-substrate interface.

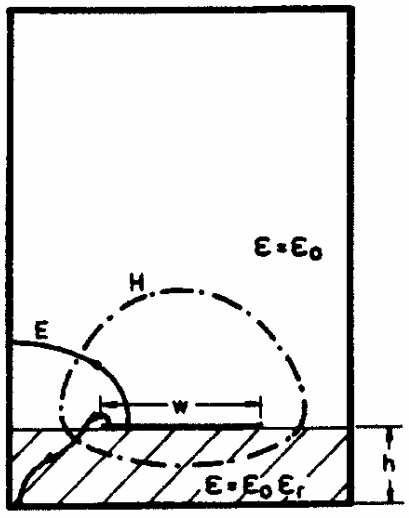

Figure 3.5: A Representative magnetic (H) and electric (E) fields of a microstrip line. Taken from Edwards and Steer [11].

3.3.4 Methods of Microstrip Analysis

The analysis methods for a microstrip lines are aimed at determining the characteristic impedance and propagation constant. It can also be used to determine the normalized ratio w/h and effective permittivity ε_{eff}. The various methods of microstrip analysis can be divided into two main groups as Quasi State Approach and Full Wave Analysis. In the Quasi State Approach the nature of the mode of propagation is considered to be pure TEM and the microstrip characteristics are calculated from the electrostatic capacitance of the structure. Full Wave Analysis takes into account the hybrid nature of the mode of propagation. The techniques followed for full wave analysis are more rigorous and analytically complex and it is not discussed here.

3.3.5 Static TEM Parameters

Methods of quasi-static analysis are used to find the static TEM parameters.

- **Characteristic Impedance Z_0.**

For any transmission line structure the basic equation for characteristics impedance is:

$$Z_0 = \sqrt{\frac{L}{C}} = v_p L = \frac{1}{v_p C}. \qquad (3.1)$$

where v_p is the phase velocity of the wave traveling along the line. L and C are the inductance and capacitance respectively per unit length for this structure. When the substrate of the microstrip line is removed we have an air filled line along which the wave will travel at c, the velocity of light in free space. The characteristic impedance for this air filled microstrip is given by

$$Z_{0a} = \sqrt{\frac{L}{C_a}} = \frac{1}{cC_a}. \qquad (3.2)$$

Where L remains unchanged by the change in the dielectric constant and C_a is the capacitance per unit length for this air filled structure.

From Equations (3.1) and (3.2) we can write

$$Z_0 = Z_{0a}\sqrt{\frac{C_a}{C}} \Rightarrow Z_0 = \frac{1}{c\sqrt{CC_a}}. \tag{3.3}$$

Thus to calculate the characteristic impedance we can calculate the capacitance per unit length of the structure with and without the dielectric substrate. There are various methods available for calculating these capacitances. These methods are not discussed here. Refer to reference section for more detail on this.

- **Effective Permittivity (ε_{eff})**

We know from the previous equations that

$$c = \frac{1}{\sqrt{LC_a}}$$

$$v_p = \frac{1}{\sqrt{LC}} \tag{3.4}$$

and $$\frac{c}{v_p} = \frac{\sqrt{LC}}{\sqrt{LC_a}} \Rightarrow \left(\frac{c}{v_p}\right)^2 = \frac{C}{C_a}. \tag{3.5}$$

The capacitance ratio C/C_a is termed as the effective microstrip permittivity.

$$\varepsilon_{eff} = \left(\frac{c}{v_p}\right)^2. \tag{3.6}$$

The upper and lower bound on the value of ε_{eff} can be easily found by considering the effects of very wide and very narrow lines as indicated in Figure 3.6.

Figure 3.6: Microstrip Lines: (a) Very wide (*w* >>*h*) and (b) Very Narrow (*w* << *h*) lines. Taken from Edwards and Steer [11].

For very wide lines the structure resembles parallel plate capacitor and all the field lines are confined to substrate dielectric. So for this case $\varepsilon_{eff} \to \varepsilon_r$. For very narrow lines the energy storage is almost shared by the air and the substrate, and for this case:

$$\varepsilon_{eff} \cong \frac{\varepsilon_r + 1}{2}. \tag{3.7}$$

Thus the range of effective permittivity is given by

$$\frac{\varepsilon_r + 1}{2} \le \varepsilon_{eff} \le \varepsilon_r. \tag{3.8}$$

The effective permittivity can also be expressed in terms of filing factor (q) as

$$\varepsilon_{eff} = 1 + q(\varepsilon_r - 1). \tag{3.9}$$

where the filing factor q is given by

$$\frac{1}{2} \le q \le 1. \tag{3.10}$$

- **Phase Velocity and Line Wavelength**

The phase velocity v_p and line wavelength λ_g are directly related to the effective permittivity:

$$v_p = c \Big/ \sqrt{\varepsilon_{eff}} \quad and \quad \lambda_g = \lambda_0 \Big/ \sqrt{\varepsilon_{eff}}. \tag{3.11}$$

Both the velocity and wavelength are functions of the transmission line's geometry and indirectly, of the characteristic impedance.

- **Width - to - Height Ratio**

The width–to–height ratio is a strong function of Z_0 and of substrate permittivity. Chapter 5 shows these results. The results are obtained with the help of Sonnet Lite® simulation.

3.3.6 Synthesis Formulas

In actual design of microstrip, one wishes to determine the width w required to obtain specified characteristic impedance Z_0 on a substrate of known permittivity ε_r

and thickness h. This operation is called synthesis. The closed synthesis formulas are highly desirable as they are very accurate and fast CAD algorithms can be implemented with these formulas. This section describes various closed formulas for microstrip calculations. All the formulas in this section are taken from Edwards & Steer [11], unless specified.

- ***Z_0* and *f* given**

For narrow strips (i.e. when $Z_0 > (44 - \varepsilon_r)\,\Omega$:

$$\frac{w}{h} = \left(\frac{\exp H'}{8} - \frac{1}{4 \exp H'} \right)^{-1} \tag{3.12}$$

where

$$H' = \frac{Z_0 \sqrt{2(\varepsilon_r + 1)}}{119.9} + \frac{1}{2}\left(\frac{\varepsilon_r - 1}{\varepsilon_r + 1} \right)\left(\ln \frac{\pi}{2} + \frac{1}{\varepsilon_r} \ln \frac{4}{\pi} \right). \tag{3.13}$$

We may also use, with slight but significant shift of changeover value to $\frac{w}{h} < 1.3$ (i.e. when $Z_0 > (60 - \varepsilon_r)\,\Omega$):

$$\varepsilon_{eff} = \frac{\varepsilon_r + 1}{2}\left[1 - \frac{1}{2H'}\left(\frac{\varepsilon_r - 1}{\varepsilon_r + 1} \right)\left(\ln \frac{\pi}{2} + \frac{1}{\varepsilon_r} \ln \frac{4}{\pi} \right) \right]^{-2}. \tag{3.14}$$

Where H' is given by Equation (3.13) (as a function of Z_0) or, alternatively, as a function of $\frac{w}{h}$, from Equation (3.12):

$$H' = \ln\left[4\frac{h}{w} + \sqrt{16\left(\frac{h}{w} \right)^2 + 2} \right]. \tag{3.15}$$

Another somewhat simpler, expression for $\varepsilon_{eff}(Z_0)$ is furnished by Equation (3.16) is :

$$\varepsilon_{eff} = \frac{\varepsilon_r + 1}{2}\left[1 + \frac{29.98}{Z_0}\left[\frac{2}{\varepsilon_r + 1} \right]\left(\frac{\varepsilon_r - 1}{\varepsilon_r + 1} \right)\left(\ln \frac{\pi}{2} + \frac{1}{\varepsilon_r} \ln \frac{4}{\pi} \right) \right]^{-2}. \tag{3.16}$$

We now consider the ranges and formulas for 'wide' strips.

For wide strips (i.e. $Z_0 < (44 - 2\varepsilon_r)\,\Omega$):

$$\frac{w}{h} = \frac{2}{\pi}\left[(d_\varepsilon - 1) - \ln\left(2d_{\varepsilon_1} - 1\right)\right] + \frac{\varepsilon_r - 1}{\pi\varepsilon_r}\left[\ln d_{\varepsilon_r} - 1 + 0.293 - \frac{0.517}{\varepsilon_r}\right] \qquad (3.17)$$

Where $d_\varepsilon = \dfrac{59.95\pi^2}{Z_0\sqrt{\varepsilon_r}}$. (3.18)

With the same slight shift of changeover value as before (i.e. where $\frac{w}{h} > 1.3$ and $Z_0 > (63 - 2\varepsilon_r)\,\Omega$) Owens found the formula:

$$\varepsilon_{eff} = \frac{\varepsilon_r + 1}{2}\frac{\varepsilon_r - 1}{2}\left[1 + 10\frac{h}{w}\right]^{-0.555}. \qquad (3.19)$$

Alternatively where Z_0 is known at first

$$\varepsilon_{eff} = \left(\frac{\varepsilon_r}{0.96 + \varepsilon_r(0.109 - 0.004\varepsilon_r)\left[\log\left(10 + Z_0\right) - 1\right]}\right). \qquad (3.20)$$

For microstrip line on alumina $(\varepsilon_r = 10)$this expression appears to be accurate to ±0.2% over the impedance range $8 \le Z_0 \le 50\Omega$.

Analysis formulas ($\frac{w}{h}$ and ε_r given)

$$Z_0 = \frac{119.9}{\sqrt{2(\varepsilon_r + 1)}}\ln\left[4\frac{h}{w} + \sqrt{16\left(\frac{h}{w}\right)^2 + 2}\right]. \qquad (3.21)$$

For wide strips ($\frac{w}{h} > 3.3$);

$$Z_0 = \frac{119.9\pi}{\sqrt{2\varepsilon_r}}\left\{\frac{w}{2h} + \frac{\ln 4}{\pi} + \frac{\ln\left(e\pi^2/16\right)}{2\pi}\left(\frac{\varepsilon_r - 1}{\varepsilon_r{}^2}\right) + \frac{\varepsilon_r + 1}{2\pi\,\varepsilon_r}\left[\ln\frac{\pi e}{2} + \ln\left(\frac{w}{2h} + 0.94\right)\right]\right\}. \qquad (3.22)$$

where e is the exponential base.

The approximate relations represented by Hammerstad and Jansen [13] in 1980 are given as follows:

$$\varepsilon_{eff} = \frac{\varepsilon_r + 1}{2} + \frac{\varepsilon_r - 1}{2}\left(1 + 10\frac{h}{w}\right)^{-ab} . \qquad (3.23)$$

where

$$a = 1 + \frac{1}{49}\log\ \frac{(w/h)^4 + (w/52h)^2}{(w/h)^4 + 0.432} + \frac{1}{18.7}\log\left\{1 + \left(\frac{1}{18.1}\frac{w}{h}\right)^3\right\}.$$

$$b = 0.564\left(\frac{\varepsilon_r - 0.9}{\varepsilon_r + 3}\right)^{0.053} .$$

The accuracy provided by these approximations is better than 0.2% for $0.01 \le w/h \le 100 \ \ and \ \ 1 \le \varepsilon_r \le 128$

3.3.7 Dispersion in Microstrip Lines

Since microstrip lines cannot support a pure TEM mode of propagation, the quasi-TEM approximation leads us to satisfactory results only below 1 or 2 GHz. As frequency increases, the energy tends to concentrate within the dielectric. The longitudinal field components increase and the hybrid character of the dominant mode becomes significant. This non-TEM behavior causes the effective dielectric constant and impedance to be functions of frequency. Of these two, the variation of the effective dielectric constant is more significant. When the frequency of a signal exciting a microstrip line is doubled, the phase constant or wave number $\beta(=2\pi/\lambda_g)$ is not exactly doubled. This phenomenon is called dispersion. This behavior is indicated in Figure 3.7.

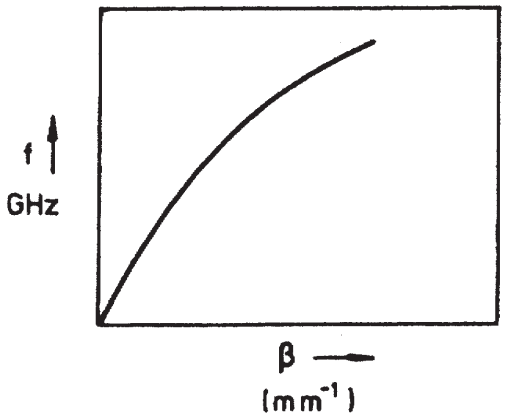

Figure 3.7: Dispersion effect in any general structure-non-linearity when frequency f is plotted against β. Taken from Edwards and Steer [11].

For microstrip lines, as frequency is increased the fields become more concentrated in the region beneath the strip, where the substrate permittivity has already resulted in a relatively large electric field displacement. As the fields are forced into the dielectric substrate to an increasing extent we can define a frequency dependent effective microstrip permittivity $\varepsilon_{eff}(f)$. This quantity increases with frequency and the wave is progressively slowed down. Thus due to dispersion of different spectral components of an information-carrying signal then propagate with different velocities, and the shape of the signal is distorted. A pulse propagating along the microstrip tends to widen as it travels. Rewriting Equation (3.11), except ε_{eff} is replaced by $\varepsilon_{eff}(f)$ and v_p by $v_p(f)$.

$$\varepsilon_{eff}(f) = \left(\frac{c}{v_p(f)} \right)^2 . \qquad (3.24)$$

Thus at the very high frequency limit, the fields are entirely contained within the dielectric, in this case the frequency dependent effective permittivity becomes the relative permittivity of the dielectric. At very low frequencies value of the

frequency dependent effective permittivity is close to the effective permittivity of the substrate. This is summarized as in Equation (3.24).

$$\varepsilon_{eff}(f) \rightarrow \begin{cases} \varepsilon_{eff} \ as \ f \rightarrow 0 \\ \varepsilon_r \quad as \ f \rightarrow \infty \end{cases} \tag{3.25}$$

Between these limits $\varepsilon_{eff}(f)$ changes continuously and this variation is shown in Figure 3.8.

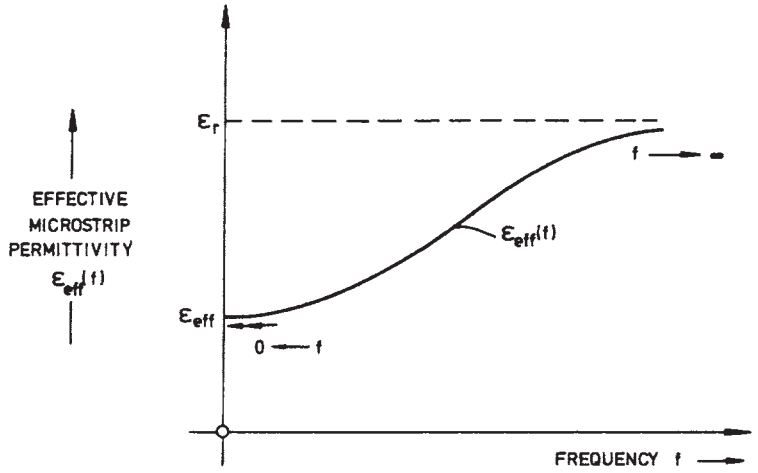

Figure 3.8: Variation of Effective Microstrip permittivity $\varepsilon_{eff}(f)$ plotted to a base of frequency. Taken from Edwards and Steer [11].

3.3.8 Expressions for Calculating ε_{eff} Accounting for Dispersion

Various researchers have developed with closed-formula for dispersion calculations. The main formulas discussed here are developed by Getsinger [1], Edwards and Owens [17], Yamashita [2], Kobayashi [3], and Kirschning & Jansen [7].

- **Getsinger's Expression**:

Getsinger [1] carried out a dynamic analysis of the field distribution in the microstrip, based on a simplified model of the microstrip: a section of parallel-plate dielectric-

loaded wave guide located between two air-filled sections. The geometric dimensions of the equivalent model were determined experimentally. A simple formula for the effective permittivity of microstrip is then obtained:

$$\varepsilon_{eff}(f) = \varepsilon_r - \left(\frac{\varepsilon_r - \varepsilon_{eff}}{1 + G\left(f / f_p \right)^2} \right) \tag{3.26}$$

where $f_p = \dfrac{Z_0}{2\mu_0 h}$. (3.27)

and μ_0 is the free-space permeability. G is purely empirical, thereby giving some flexibility to the formula. G is dependent mainly upon Z_0, but also to a lesser extent upon h, and Getsinger deduced from measurements of microstrip ring resonators on alumina that

$$G = 0.6 + 0.009 Z_0 \tag{3.28}$$

- **Edwards and Owens Expression**

Edwards and Owens [17] suggested the following expression for dispersion:

$$\varepsilon_{eff}(f) = \varepsilon_r - \left(\frac{\varepsilon_r - \varepsilon_{eff}}{1 + \left(h / Z_0 \right)^{1.33} \left(0.43 f^2 - 0.009 f^3 \right)} \right). \tag{3.29}$$

where h is in millimeters and f is in gigahertz.

The design expressions presented by Getsinger and Edwards and Owens are well tested and checked against experimental measurements for frequencies up to approximately 18GHz. This frequency is, however, far below the limits at which microstrip can be used – up to the vicinity of 100GHz at least – as there are increasing applications available for MICs and MMICs at millimeter wave frequencies. It has therefore long been recognized that a requirement exists for closed formulas that would enable calculations to be conducted including dispersion in microstrip at these high frequencies. There main formulas discussed here for high frequencies are developed by Yamashita, Kobayashi, and Kirschning & Jansen.

- **Yamashita's Expression**

Yamashita's approximate dispersion formula [2] covering the frequency range 1 to 100 GHz is given by:

$$\varepsilon_{eff}(f) = \left(\frac{\sqrt{\varepsilon_r} - \sqrt{\varepsilon_{eff}}}{1 + 4F^{-1.5}} + \sqrt{\varepsilon_{eff}} \right)^2 \tag{3.30}$$

where $F = \frac{4hf\sqrt{\varepsilon_r - 1}}{c} \left[0.5 + \left\{ 1 + 2\log\left(1 + \frac{w}{h}\right) \right\}^2 \right]$. (3.31)

However this expression is not particularly accurate – especially in the lower frequency range up to 18GHz, where the expression due to Edwards and Owens is recommended. The formula is applicable in the range of $2 \le \varepsilon_r \le 16,\ 0.06 \le w/h \le 16$ and $f \le 100GHz$.

- **Kobayashi's Expression:**

Kobayashi's work [3] was based upon the concept of a significant 50% dispersion point, a frequency at which the effective microstrip permittivity is the arithmetic mean of the substrate relative permittivity and the low frequency limit value. The dispersion formula is given in Equation (3.32).

$$\varepsilon_{eff}(f) = \varepsilon_r - \left(\frac{\varepsilon_r - \varepsilon_{eff}}{1 + \left(f / f_{50}\right)^m} \right) \tag{3.32}$$

where

$$f_{50} = \frac{f_{k,TM_0}}{0.75 + \left[0.75 - \left(0.332 / \varepsilon_r^{1.73} \right) \right] w/h}.$$

$$f_{k,TM_0} = \frac{c \tan^{-1}\left(\varepsilon_r \sqrt{\frac{\varepsilon_{eff} - 1}{\varepsilon_r - \varepsilon_{eff}}} \right)}{2\pi h \sqrt{\varepsilon_r - \varepsilon_{eff}}}.$$

$$m = m_0 m_c.$$

$$m_0 = 1 + \frac{1}{1+\sqrt{\frac{w}{h}}} + 0.32\left(\frac{1}{1+\sqrt{w/h}}\right)^3 .$$

$$m_c = \begin{cases} 1 + \dfrac{1.4}{1+w/h}\left[0.15 - 0.235\ \exp\left(\dfrac{-0.45f}{f_{50}}\right)\right] & when\ \ w/h \le 0.7 \\ 1 & when\ \ w/h > 0.7 \end{cases}$$

The range of the formula is $1 \le \varepsilon_r \le 128$ and $0.1 \le w/h \le 10$.

- **Kirschning and Jansen's Expression**

Kirschning and Jansen [7] have developed an improved design formula. Their approach begins with a function that bears a close resemblance to Getsinger's but they have a new and reportedly more accurate frequency dependent denominator term. Also their formula covers a much wider range of permittivity, aspect ratios and frequencies than those considered by Getsinger or Edwards and Owens.

This expression is given as in Equation (3.33) (with frequency f in GHz and thickness h in cm):

$$\varepsilon_{eff}(f) = \varepsilon_r - \left(\frac{\varepsilon_r - \varepsilon_{eff}}{1+P(f)}\right) \qquad (3.33)$$

Now the form of the denominator frequency function is

$$P(f) = P_1 P_2 \left\{(0.1844 + P_3 P_4)10fh\right\}^{1.5763} \text{ where}$$

$$P_1 = 0.27488 + \left[0.6315 + 0.525/(1+0.157fh)^{20}\right](w/h) - 0.065683\ \exp(-8.7513\,w/h)$$

$$P_2 = 0.33622\left[1 - \exp\left(-0.03442\varepsilon_r\right)\right].$$

$$P_3 = 0.0363\ \exp(-4.6\,w/h)\left\{1 - \exp\left[-(fh/3.87)^{4.97}\right]\right\}.$$

$$P_4 = 1 + 2.751\left\{1 - \exp\left[-(\varepsilon_r/15.916)^8\right]\right\}.$$

The validity range is very wide

$$1 \le \varepsilon_r \le 20,\ 0.1 \le w/h \le 100,\ 0 \le h/\lambda_0 \le 0.13 .$$

3.4 Summary

This chapter described the microstrip lines in detail. Various design formulas and dispersion formulas for microstrip lines are mentioned here. These formulas will be used later in Chapter 5, while summarizing the results.

Chapter 4

Sonnet Lite

4.1 About Sonnet Lite®

Sonnet® Software provides commercial EDA software solutions for high frequency electromagnetic analysis. This electromagnetic simulation software is used for design and analysis of high frequency circuits, distributed filters, transitions, LTCC and multi layer RF packages, wave guides and antennas.

4.2 Capabilities

Sonnet Lite® is a feature limited registered version of the Sonnet Professional Suite®. Sonnet Lite® contains many of the features and capabilities of Sonnet Professional®, using the same user interface and analysis engine. The analysis engine of the Sonnet Suite®, Em, performs electromagnetic analysis for arbitrary 3–D planar (e.g., microstrip, coplanar, strip line, etc.) geometries, maintaining full accuracy at all frequencies. Em is a “full-wave” analysis in that it takes into account all possible coupling mechanisms. The analysis inherently includes dispersion, stray coupling, discontinuities, surface waves, moding, metallization loss, dielectric loss and radiation loss. In short, it is a complete electromagnetic analysis. Since Em uses a surface meshing technique, i.e. it meshes only the surface of the circuit metallization, Em can analyze predominately planar circuits much faster than volume meshing techniques.

Em does what is called a 2 and half dimensional analysis that includes 3–D fields but imposes a restriction on the currents. Currents must be either in the plane of the conductors (x–y directed) or vertical (z directional). This is a very good approximation for planar interconnects with vertical vias. Em analyzes 3–D structures embedded in planar multilayered dielectric on an underlying fixed grid. For this class of circuits, Em can use the FFT (Fast Fourier Transform) analysis

technique to efficiently calculate the electromagnetic coupling on and between each dielectric surface. This provides Em with several orders of magnitude speed increase relative to electromagnetic analysis utilizing volume tric meshing and other non FFT based surface meshing techniques.

Table 4.1: Capabilities of Sonnet Lite® .

Feature	Sonnet Lite®	Sonnet Professional®
Analysis Memory Allowed	16 MB	Unlimited
Metal Layers Allowed	2 + GND	Unlimited
Circuit Ports	4	Unlimited
Box Resonance Detection	✓	✓
Via modeling	✓	✓
Circuit Parameters	✓	✓
Hybrid Net lists	✓	✓
Adaptive Band Synthesis (ABS)	✓	✓
Internal Ports		✓
Palette of Standard Geometries		✓
Circuit Optimization		✓
Automated User Guided Circuit Subdivision		✓
DXF Translator (import/export)		✓
GDSII Translator (import/export)		✓
Far field Radiation Pattern Display		✓
OS Supported	PC Windows	PC Windows, Solaris (Sun), HP-UX

4.3 How does the Sonnet Suite® work?

The suite of Sonnet® analysis tools is shown in Figure 4.1. Using these tools, Sonnet® provides an open environment to many other design and layout programs. The following is a brief description of all of the Sonnet tools®.

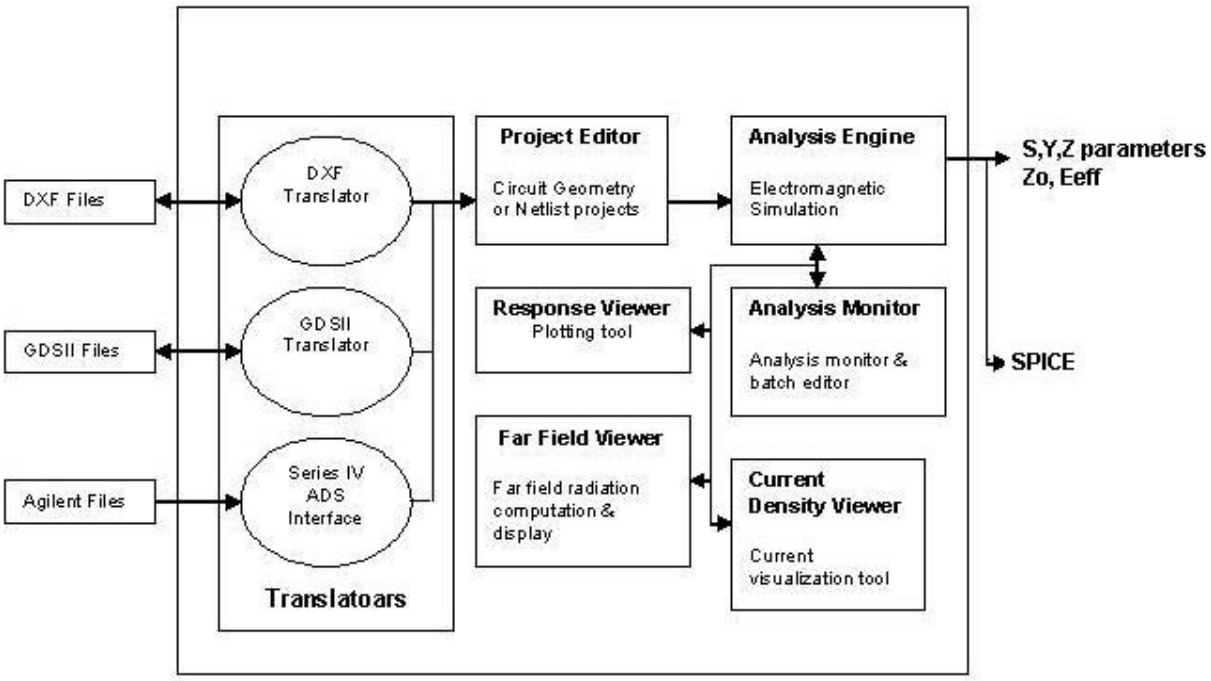

Figure 4.1: How does the Sonnet suite® works?

Project Editor: The project editor is a user friendly graphical interface that enables the user to input a circuit geometry or circuit net list for subsequent Em analysis. Analysis controls for the project are set up in the project editor.

Analysis Engine: Em is the electromagnetic analysis engine. It uses a modified method of moments analysis based on Maxwell's equations to perform a true three-dimensional current analysis of predominantly planar structures. Em computes S, Y, or Z–parameters, transmission line parameters (Z_0 and ε_{eff}), and SPICE equivalent lumped element networks. Additionally, it creates files for further processing by the current density viewer and the far field viewer. Using Sonnet's net list, Em cascades the results of electromagnetic analyses with lumped elements, ideal transmission line elements and external S–parameter data. For more information about Em, see the Sonnet User's Guide.

Analysis Monitor: The analysis monitor allows you to observe the on going status of analyses being run by Em as well as creating and editing batch files to provide a queue for Em jobs.

Response Viewer: The response viewer is the plotting tool. This program allows you to plot your response data from Em, as well as other simulation tools, as a Cartesian graph or a Smith chart.

Current Density Viewer: The current density viewer is a visualization tool, which acts as a post processor to Em providing you with an immediate qualitative view of the electromagnetic interactions occurring within your circuit.

Far Field Viewer: The far field viewer is the radiation pattern computation and display program It computes the far field radiation pattern of radiating structures (such as patch antennas) using the current density information from Em and displays the far field radiation patterns in one of three formats: Cartesian plot, polar plot or surface plot.

GDSII Translator: The GDSII translator provides bi directional translation of GDSII layout files to/ from the Sonnet project editor geometry format.

DXF Translator: The DXF translator provides bi directional translation of DXF layout files (such as from AutoCAD) to/from the Sonnet project editor geometry format.

Agilent Interface: The Agilent Interface provides a seamless translation capability between Sonnet and Agilent Series IV and Agilent ADS. From within the Series IV or ADS Layout package you can directly create Sonnet geometry files. Em simulations can be invoked and the results incorporated into your design without leaving the Series IV or ADS environment.

4.4 Analysis Memory Limits

Sonnet Lite® is limited to the size of the circuit it can analyze. Larger, more complex circuits require more memory to analyze. Sonnet Lite® is limited to 1 MB when it is first installed, but you may increase that limit to 16 MB by registering. Registration is free.

4.5 Applications

Em is appropriate for a wide range of 3–D planar structures. The via capability allows the analysis of air bridges, wire bonds, spiral inductors, wafer probes and internal ports as well as for simple grounding. It is appropriate to use **Em** for the evaluation of specific discontinuities or groups of interacting discontinuities to assist in the design of a 3–D planar circuit

Em provides ultra precise S–parameters for discontinuities allowing designers to work with confidence. Em can also quickly synthesize an equivalent lumped model for discontinuities. The lumped model can be used directly in circuit theory programs.

Design validation

Using Em for design validation effectively eliminates expensive design iterations (i.e., “tweak”, re-fabricate, etc.) of the passive, planar portion of a circuit. If a circuit is designed from the start with electromagnetic analysis in mind, larger circuits can be done. For example, the analysis works best with tightly packed, rectangular circuits, designed on a common dimension grid.

Microwave package evaluation

It is important to assess how a circuit will operate in the package environment. Em analyzes a circuit inside a conducting box. If the box (acting as a dielectric loaded resonator) is resonant at a frequency where the circuits still have gain, poor performance results. Em provides an analysis of a package prior to fabrication. Resonances can then be dealt with on the computer rather than on the test bench.

Microstrip antennas

The “top” of Em’s box can be effectively removed. While radiation is outside of Em’s primary thrust, a wide variety of microstrip antennas and radiating discontinuities can be evaluated.

High speed digital interconnect

When an approximate model is not good enough, Em can synthesize a SPICE lumped model including all delays and couplings. The lumped model is synthesized directly from electromagnetic data.

Em is not appropriate for doing an initial design. Rather, the faster circuit theory simulators (which do not typically include stray coupling) should be used for the first cut. Em can then enhance the simulator performance by providing custom, ultra precise discontinuity data and by validating large portions of the final circuit, including all stray interactions. Em is designed to work with any existing CAE software. Since Em allows the user to choose from a wide range of standard output formats, Em provides a seamless interface to any CAE tool.

4.6 Version Used

In this thesis the latest version Sonnet Lite 8® is used. It retains the popular features enjoyed by customers in the Release 7 version, such as:

- Parametric geometry control
- Geometry sweep analysis
- Analysis of circuits with up to 4 ports and 2 signal + 2 ground (top/bottom) levels.

Chapter 5

Simulation and Results

5.1 Introduction

This chapter describes the simulation results obtained from Sonnet Lite® for microstrip lines. These simulation results are useful for plotting various curves for microstrip design formulas and dispersion in microstrip lines. These results are also compared with the curves obtained by the mathematical (synthesis) formulas. These curves are plotted in Microsoft excel. The curves also show various trends in microstrip circuit design.

5.2 Simulation

The main design problem in all microstrip designs is to evaluate the physical widths and lengths of the microstrip lines. Width of the microstrip line is principally a function of its characteristic impedance and the thickness of the substrate. The physical length depends upon the wavelength, which is a function of the width, the substrate permittivity, and of course, the signal frequency. So various results relating characteristic impedance, effective permittivity and width/height ratio are described in this section.

5.2.1 Drawing a geometry in Sonnet Lite®

This section describes the basic steps for drawing any geometry in Sonnet Lite®, along with the geometry of a microstrip line, which is used to analyze microstrip design curves. Following are the steps for drawing geometry in Sonnet Lite®.

If you wish to manually enter new circuit geometry in the project editor, you must first create a new project. To do so, select File → New Geometry from the project editor main menu. This opens a new geometry project with a blank substrate. The screen will look like that shown in Figure 5.1.

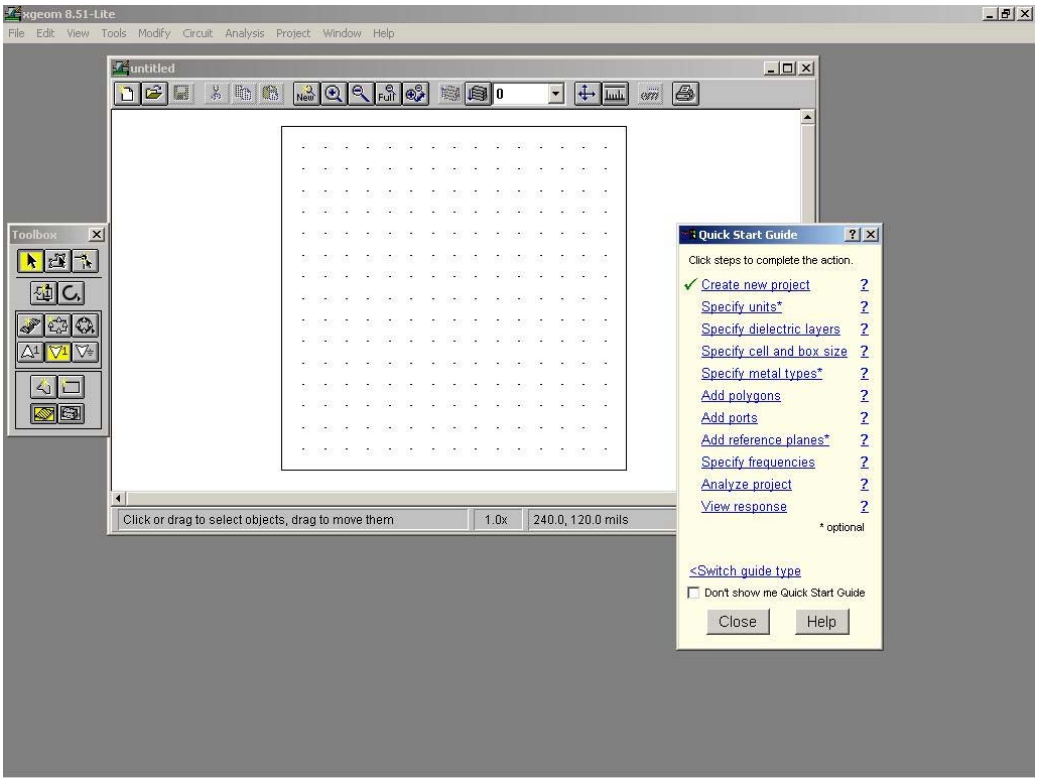

Figure 5.1: New geometry project with blank substrate in Sonnet Lite®

Before entering the circuit in the project editor, you should input what length and frequency units to use for your geometry. It is possible to change the units later if needed, so that this is an optional step in importing or creating a circuit. Units are available for Length, Frequency, Resistance, Inductance and Capacitance. Resistance, Inductance and Capacitance units are only available for Net list projects.

Length: Units available are mils, microns, mm, cm, inches and meters. The default length unit in a new project is mils.

Frequency: Units available are Hz, kHz, MHz, GHz, THz, and PHz. The default frequency unit is GHz.

Resistance: Units available are Ohms, kOhms, and MOhms. The default resistance unit is Ohms.

Inductance: Units available are H, mH, μH, nH, pH, and fH. The default inductance is nH.

Capacitance: Units available are F, mF, μF, nF, pF, and fF. The default is pF.

The units used here are frequency in GHz and length in mm. The dialogue box is as shown in Figure 5.2.

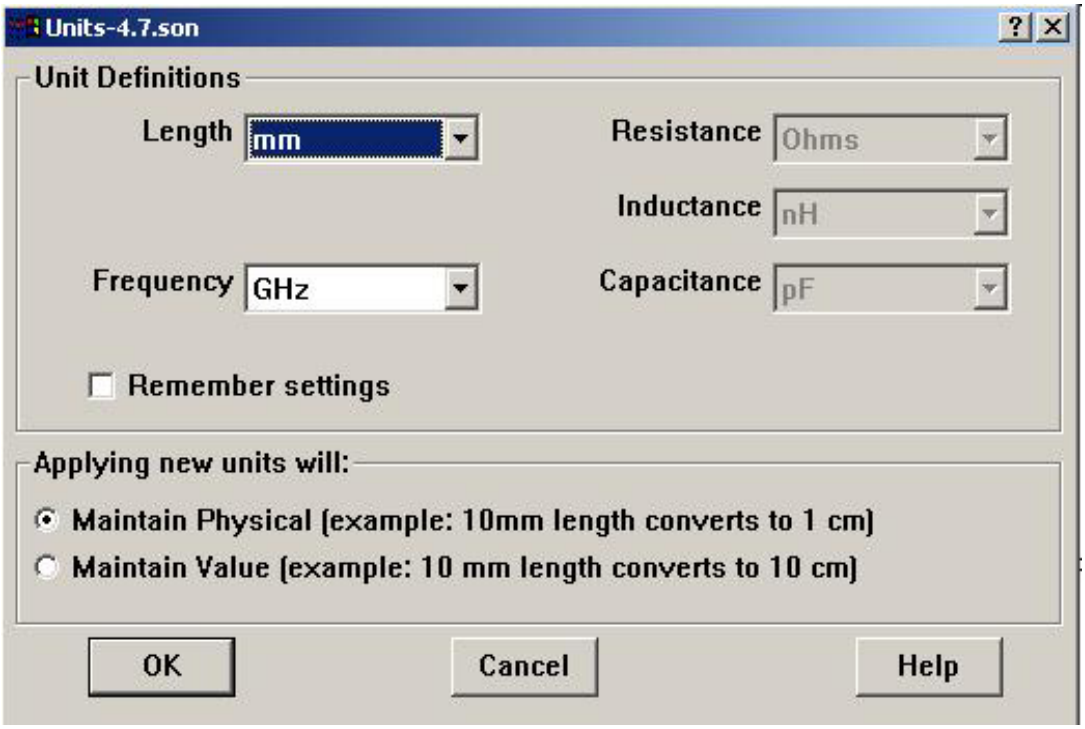

Figure 5.2: Dialogue Box for choosing units for any geometry.

- **Specify Dielectric Layers**

The next step is to specify the dielectric layers, which includes the substrate, for your circuit. Each dielectric layer has a metal level associated with it where the metallization of the circuit is placed. The circuit geometry consists of alternate

dielectric layers and metal levels enclosed in a six sided metal box. Each time a dielectric layer is added a metal level is added.

The example below in Figure 5.3 is a 3–dimensional drawing of a circuit (with the Z-axis exaggerated) on the left side with the dielectric layers dialog box for the same circuit shown on the right. It is important to note that the metal level is associated with the dielectric layer above it. If that dielectric layer is deleted from the circuit, then the metallization below it is also deleted. For example, if you deleted the dielectric layer between metal levels 1 and 2 in Figure 5.3 shown below, the level 2 metallization would also be removed. The type of dielectric is specified for each dielectric layer by entering the dielectric constant and loss parameters for each layer in the dielectric layers dialog box.

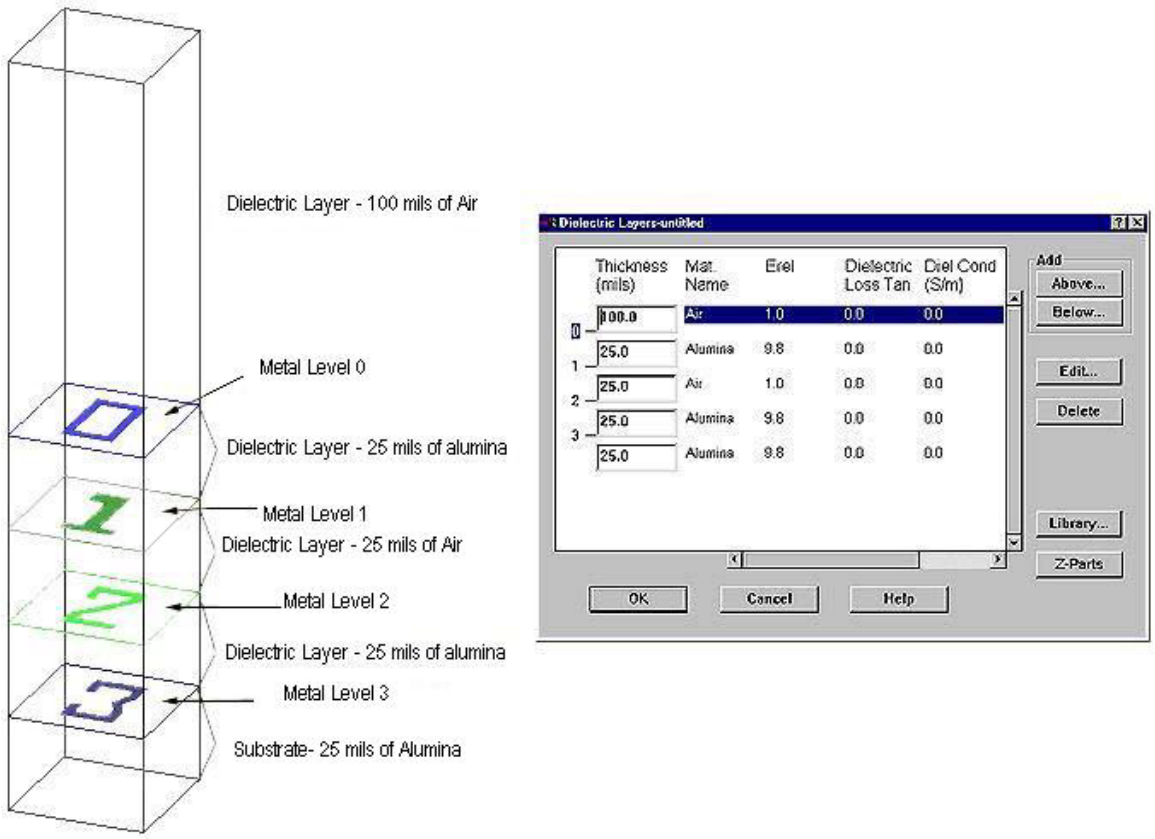

(a) **(b)**

Figure 5.3: Specifying dielectric layers in the dielectric layers dialog box: (a) 3 dimensional drawing of a circuit; and (b) dialog box dielectric layers. Taken from Sonnet User's Guide [18].

Here for the microstrip line there is only one dielectric layer. The dialogue box for entering the values of dielectric layer is as shown in Figure 5.4.

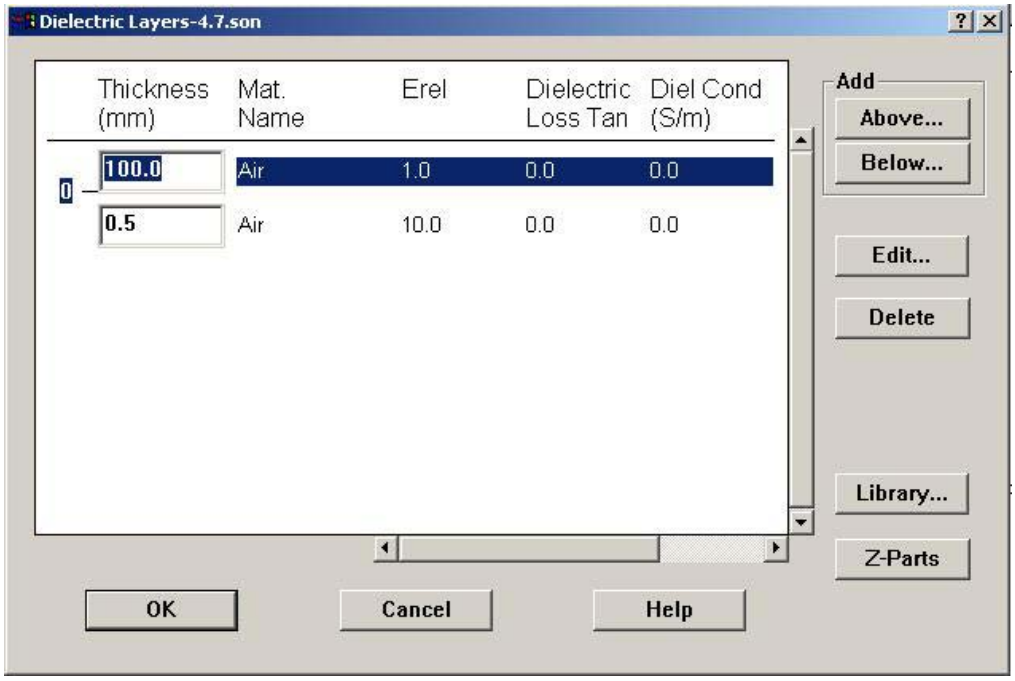

Figure 5.4: The dielectric layers dialogue box.

- **Specify cell and box size**

Sonnet considers that a circuit is in a six sided enclosure. Entering the box size, along with the dielectric layers, determines the box size. The cell size controls how the circuit is sub sectioned for analysis and may be used to set the grid for the circuit. You must have an integer number of cells for each dimension of the box bottom and top; however, the cell size does not have to be an integer value.

What is the Box?

Sonnet analyzes planar structures inside a six sided shielding box. It is as shown in Figure 5.5. Port connections are usually made at the box sidewalls. The substrate viewed in the project editor is on the bottom of the box with dielectric layers and metal levels stacked above it. The sidewalls of the box are modeled as loss less metal. The top and bottom of the box may be assigned any metal type defined in the geometry project.

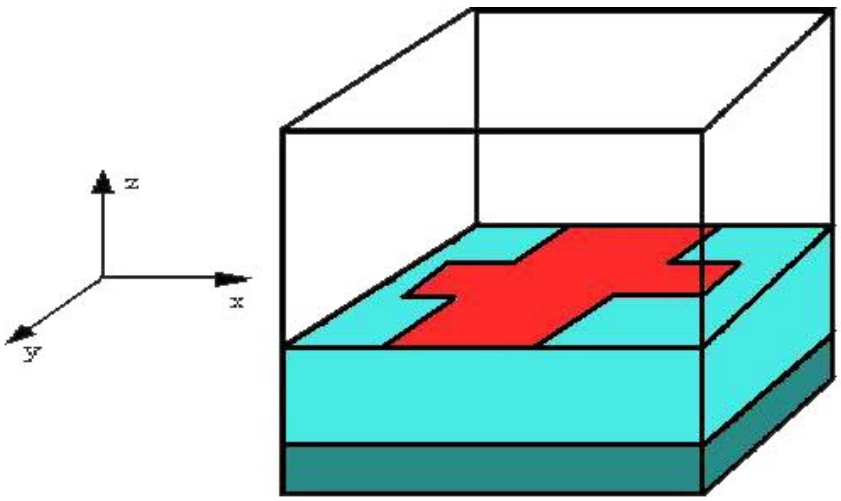

Figure 5.5: Typical box in Sonnet Lite®

What is a Cell?

The electromagnetic analysis starts by automatically subdividing a circuit into small rectangular subsections. Em uses variable size subsections: small subsections are used where needed and larger subsections are used where the analysis does not need small subsections.

A “cell” is the basic building block of all subsections, and each subsection is “built” from one or more cells. Thus a subsection may be as small as one cell or may be multiple cells long or wide. Thus the “dimensions” of a cell determine the minimum subsection size. The smaller the subsections are made, the more accurate the result is and the longer it takes to get the result. Therefore, there is a trade off between accuracy and processing time to be considered when choosing the cell size. The project editor gives you a measure of control over the subsection size. Note that the dimensions of a cell need not be a “round” number. For example, if you want to analyze a line that is 9.5 mils wide, you need not set your cell dimension to 0.5 mils. You may want to set it to 4.75 mils (9.5 mils divided by 2) or 3.16667 mils

(9.5 mils divided by 3). This will speed up the analysis because fewer subsections will be used. Also, the width of the cell does not need to be the same as the length. When viewing your substrate, notice that the project editor displays a grid made up of regularly spaced dots. The distance between each grid point is the cell size. There is also cell size calculator for calculating the cell size.

For this microstrip geometry, the dialogue box is as shown in Figure 5.6.

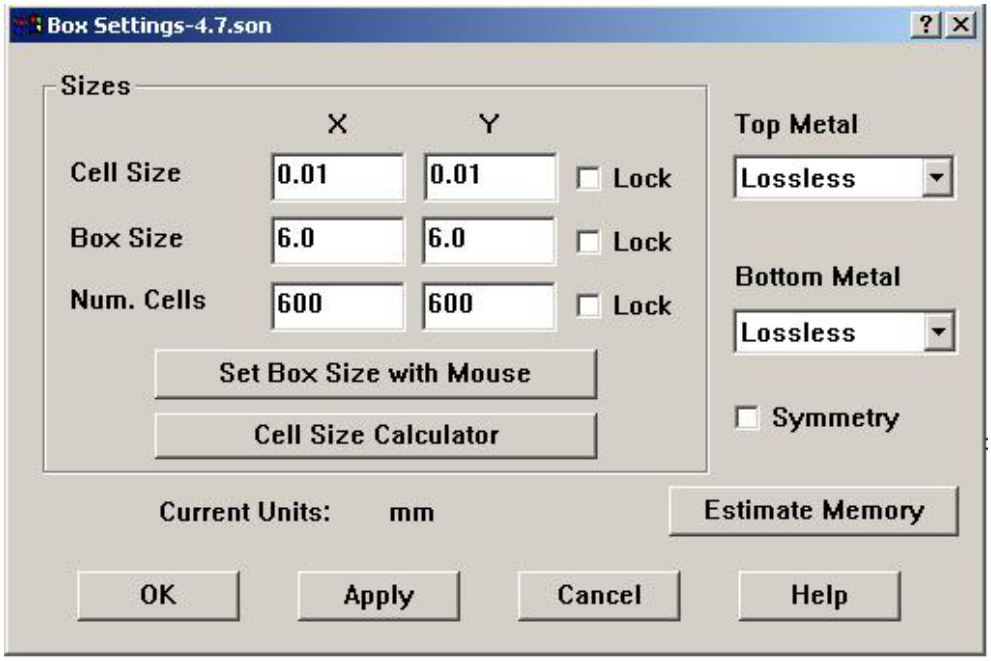

Figure 5.6: Box settings for microstrip geometry.

- **Specify the metal types**

Every new circuit geometry in Sonnet has one metal, Loss less, defined. If that is the only metal you wish to use, you may skip this step. However, if you wish to define

additional metals for use in your circuit, you may do so. Here for the microstrip geometry this step is skipped.

- **Add a rectangle**

Selecting the Add a Rectangle button in the project editor's toolbox provides you with a quick way to create rectangular polygons. The polygon is metal or dielectric brick depending on which mode is selected in the toolbox.

- **Add a port**

There are four kinds of port we can add in Sonnet.

- Standard box wall port
- Ungrounded internal port
- Via port
- Auto grounded port.

The port added here in this microstrip geometry is standard box wall port. A standard box wall port is a grounded port, one terminal attached to a polygon edge coincident with a box wall and the second terminal attached to ground.

- **Specify frequency & analysis type**

You must input the set of frequencies at which you wish to analyze your circuit. The simplest type of analysis in Sonnet is the Linear Frequency Sweep. There are also some other types of analysis available. They are Adaptive Sweep (ABS), Frequency Sweep Combinations, Parameter Sweep, Optimization and External Frequency File.

Parameter sweep:

It is often necessary to perform several iterations of a circuit design in order to meet specifications. Part of those iterations involves changing the dimensions or attributes of some part of your circuit. Parameterization and optimization can be used to make this task more efficient. Rather than create multiple circuits each with different lengths of key components, you may select dimensions of your circuit and define them as a parameter. In the analysis, you automatically vary the value of the parameter rather than setting up a separate circuit file for each value.

Parameterizing your circuit also provides you with a way to quickly and easily change dimensions in the project editor. In a parameter sweep, the analysis engine, Em, adjusts the value of a parameter by sweeping the parameter values through a user defined range. A parameter sweep of geometry may be performed over a range of analysis frequencies. The same concept is used here. Here the width of the microstrip line from 0.05 to 4 mm at the increment of 0.2mm. And the range of analysis frequency is 1–10 GHz. The purpose of varying the width is we will get the variation of ε_{eff}, Z_0 and q as a function of w/h. The dialogue box for the analysis setup will look shown in Figure 5.7.

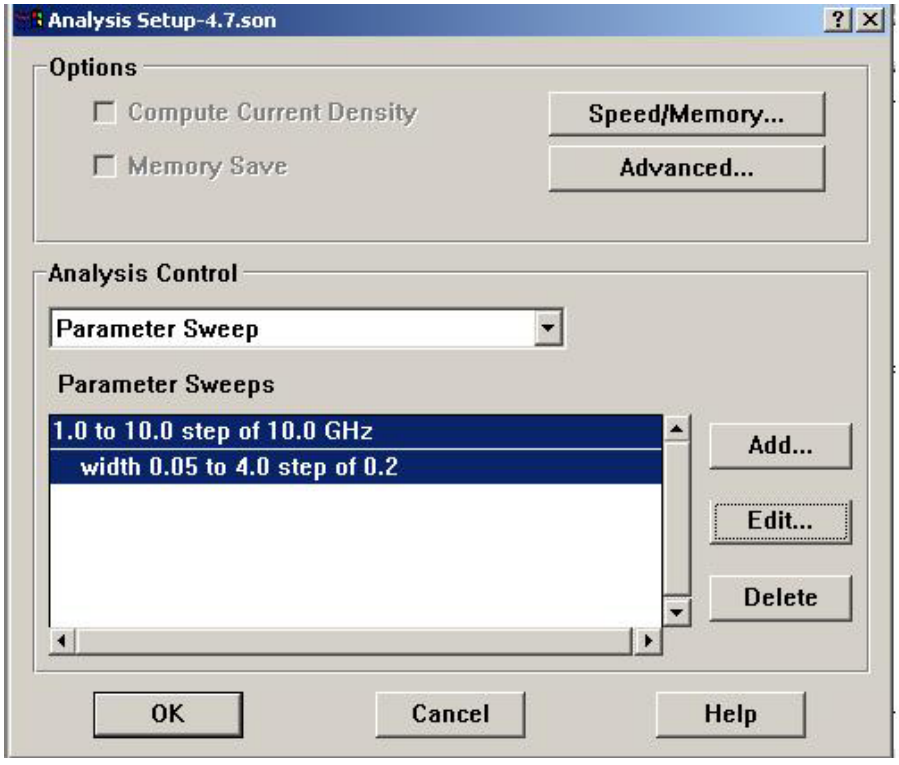

Figure 5.7: Dialogue box for analysis setup of microstrip geometry.

The final geometry of microstrip line will look like shown in Figure 5.8. For more information on drawing geometry in Sonnetlite® and how Sonnetlite® works refer to the cited reference[18].

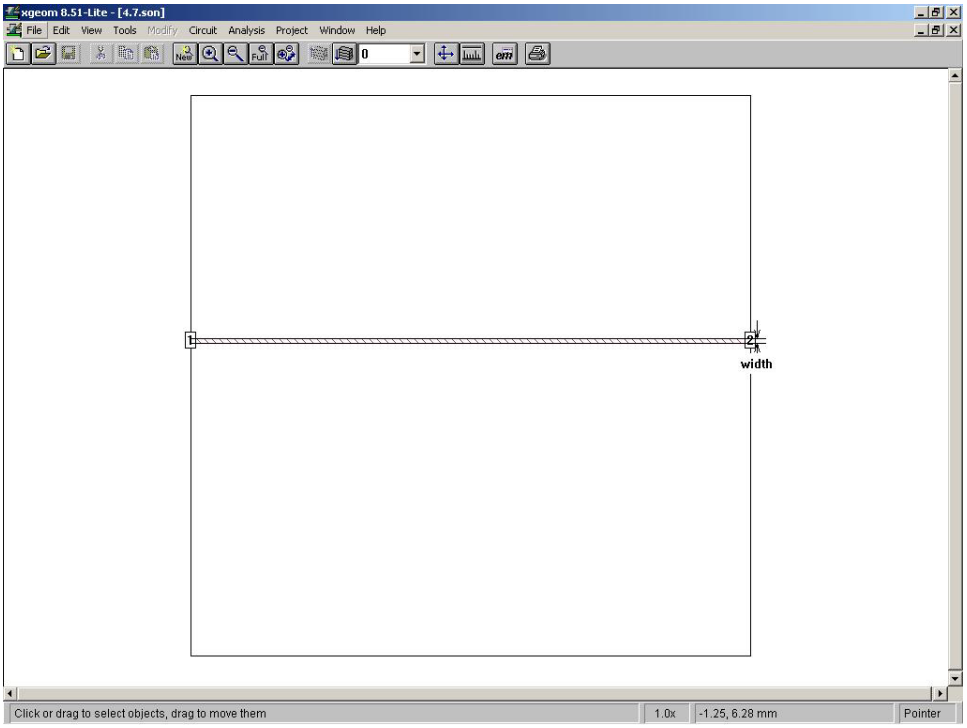

Figure 5.8: Final geometry of a Microstrip Line in Sonnet Lite.

5.3 Results

5.3.1 Microstrip Design Curves

Through parameter sweep sonnet simulation gives us the values of Effective permittivity (ε_{eff}), Characteristics Impedance (Z_0) at frequencies 1GHz & 10 GHz for different aspect ratio. Relative permittivity (ε_r) of the material can be changed as shown in Figure 5.4.

So, from sonnet simulation the values of ε_{eff} and Z_0 for various values of ε_r were obtained. Thus Table 5.1, 5.2, 5.3 & 5.4 shows values of ε_{eff}, q and Z_0 for different aspect ratios at 1GHz. Various values chosen for ε_r are 1, 2,4,6,10,20 and 40.

Value of q (filing factor) is calculated as follows:

$$\varepsilon_{eff} = 1 + q(\varepsilon_r - 1) \Rightarrow q = \left(\varepsilon_{eff} - 1\right) \Big/ (\varepsilon_r - 1)$$

The results of the simulations are tabulated in Tables 5.1–5.4.

Table 5.1: Variation of Z_0, ε_{eff}, q for different w/h ratio and ε_r =1 & 2 at frequency 1GHz.

ε_r =1				ε_r =2			
w/h	Z_0	ε_{eff}	q	w/h	Z_0	ε_{eff}	q
0.05	267.2817	1.0037		0.05	214.0128	1.5655	0.5655
0.25	167.4246	1.0055		0.25	132.4720	1.6061	0.6061
0.45	131.9737	1.0066		0.45	103.5870	1.6340	0.6340
0.65	110.8543	1.0076		0.65	86.4472	1.6569	0.6569
0.85	96.2065	1.0084		0.85	74.6181	1.6765	0.6765
1.05	85.2653	1.0092		1.05	65.8288	1.6932	0.6932
1.25	76.7002	1.0099		1.25	58.9848	1.7076	0.7076
1.45	69.7778	1.0105		1.45	53.4818	1.7202	0.7202
1.65	64.0447	1.0110		1.65	48.9462	1.7311	0.7311
1.85	59.2061	1.0116		1.85	45.1360	1.7405	0.7405
2.05	55.0582	1.0120		2.05	41.8838	1.7487	0.7487
2.25	51.4552	1.0123		2.25	39.0707	1.7559	0.7559
2.45	48.2908	1.0126		2.45	36.6098	1.7620	0.7620
2.65	45.4840	1.0129		2.65	34.4357	1.7671	0.7671
2.85	42.9724	1.0131		2.85	32.4978	1.7714	0.7714
3.05	40.7066	1.0132		3.05	30.7564	1.7749	0.7749
3.25	38.6462	1.0133		3.25	29.1793	1.7775	0.7775
3.45	36.7584	1.0134		3.45	27.7405	1.7793	0.7793
3.65	35.0146	1.0133		3.65	26.4174	1.7802	0.7802
3.85	33.3890	1.0132		3.85	25.1901	1.7802	0.7802

Table 5.2: Variation of Z_0, ε_{eff}, q for different w/h ratio and ε_r =4 & 6 at frequency 1GHz.

ε_r =4				ε_r =6			
w/h	Z_0	ε_{eff}	q	w/h	Z_0	ε_{eff}	q
0.05	163.6510	2.6774	0.5591	0.05	137.6262	3.7858	0.5572
0.25	100.4713	2.7923	0.5974	0.25	84.2207	3.9739	0.5948
0.45	78.1221	2.8730	0.6243	0.45	65.3393	4.1072	0.6214
0.65	64.8976	2.9402	0.6467	0.65	54.1785	4.2187	0.6437
0.85	55.8021	2.9977	0.6659	0.85	46.5138	4.3145	0.6629
1.05	49.0697	3.0473	0.6824	1.05	40.8490	4.3973	0.6795
1.25	43.8473	3.0903	0.6968	1.25	36.4613	4.4691	0.6938
1.45	39.6630	3.1276	0.7092	1.45	32.9510	4.5316	0.7063
1.65	36.2262	3.1601	0.7200	1.65	30.0716	4.5861	0.7172
1.85	33.3481	3.1885	0.7295	1.85	27.6633	4.6336	0.7267
2.05	30.8987	3.2132	0.7377	2.05	25.6161	4.6751	0.7350
2.25	28.7860	3.2347	0.7449	2.25	23.8522	4.7112	0.7422
2.45	26.9427	3.2532	0.7511	2.45	22.3149	4.7425	0.7485
2.65	25.3184	3.2690	0.7563	2.65	20.9615	4.7692	0.7538
2.85	23.8742	3.2823	0.7608	2.85	19.7593	4.7917	0.7583
3.05	22.5797	3.2931	0.7644	3.05	18.6828	4.8102	0.7620
3.25	21.4105	3.3015	0.7672	3.25	17.7114	4.8246	0.7649
3.45	20.3466	3.3075	0.7692	3.45	16.8284	4.8350	0.7670
3.65	19.3711	3.3109	0.7703	3.65	16.0197	4.8411	0.7682
3.85	18.4691	3.3116	0.7705	3.85	15.2728	4.8427	0.7685

Table 5.3: Variation of Z_0, ε_{eff}, q for different w/h ratio and ε_r =10 & 20 at frequency 1GHz.

ε_r =10				ε_r =20			
w/h	Z_0	ε_{eff}	q	w/h	Z_0	ε_{eff}	q
0.05	109.3213	6.0003	0.5556	0.05	78.8451	11.5355	0.5545
0.25	66.7111	6.3342	0.5927	0.25	48.0013	12.2344	0.5913
0.45	51.6524	6.5727	0.6192	0.45	37.1053	12.7367	0.6177
0.65	42.7602	6.7731	0.6415	0.65	30.6763	13.1604	0.6400
0.85	36.6611	6.9458	0.6606	0.85	26.2712	13.5262	0.6593
1.05	32.1590	7.0953	0.6773	1.05	23.0234	13.8437	0.6760
1.25	28.6770	7.2252	0.6917	1.25	20.5140	14.1198	0.6905
1.45	25.8946	7.3383	0.7043	1.45	18.5108	14.3605	0.7032
1.65	23.6151	7.4370	0.7152	1.65	16.8714	14.5707	0.7142
1.85	21.7103	7.5233	0.7248	1.85	15.5027	14.7547	0.7239
2.05	20.0932	7.5986	0.7332	2.05	14.3417	14.9156	0.7324
2.25	18.7011	7.6643	0.7405	2.25	13.3429	15.0559	0.7398
2.45	17.4888	7.7212	0.7468	2.45	12.4739	15.1777	0.7462
2.65	16.4225	7.7700	0.7522	2.65	11.7100	15.2823	0.7517
2.85	15.4761	7.8112	0.7568	2.85	11.0324	15.3711	0.7564
3.05	14.6293	7.8452	0.7606	3.05	10.4266	15.4441	0.7602
3.25	13.8659	7.8719	0.7635	3.25	9.8808	15.5021	0.7633
3.45	13.1726	7.8913	0.7657	3.45	9.3854	15.5444	0.7655
3.65	12.5381	7.9030	0.7670	3.65	8.9325	15.5708	0.7669
3.85	11.9528	7.9066	0.7674	3.85	8.5150	15.5796	0.7673

Table 5.4: Variation of Z_0, ε_{eff}, q for different w/h ratio and ε_r =40 at frequency 1GHz.

ε_r =40			
w/h	**Z_0**	**ε_{eff}**	**q**
0.05	56.3179	22.6120	0.5542
0.25	34.2407	24.0467	0.5909
0.45	26.4430	25.0816	0.6175
0.65	21.8442	25.9563	0.6399
0.85	18.6950	26.7130	0.6593
1.05	16.3747	27.3705	0.6762
1.25	14.5829	27.9429	0.6908
1.45	13.1536	28.4423	0.7036
1.65	11.9845	28.8791	0.7148
1.85	11.0090	29.2615	0.7247
2.05	10.1817	29.5960	0.7332
2.25	9.4705	29.8882	0.7407
2.45	8.8518	30.1420	0.7472
2.65	8.3083	30.3604	0.7528
2.85	7.8264	30.5457	0.7576
3.05	7.3957	30.6989	0.7615
3.25	7.0078	30.8205	0.7646
3.45	6.6559	30.9102	0.7669
3.65	6.3342	30.9663	0.7684
3.85	6.0379	30.9865	0.7689

The data provided in Tables 5.1, 5.2, 5.3, 5.4 are plotted with the help of Microsoft Excel so that we can better understand and analysis the effects of variation of w/h ratio on ε_{eff}, Z_0 and q for various dielectric materials (for different values of ε_r).

The plot shown in Figure 5.9 shows the variation of Z_0 with respect to aspect ratio (w/h).

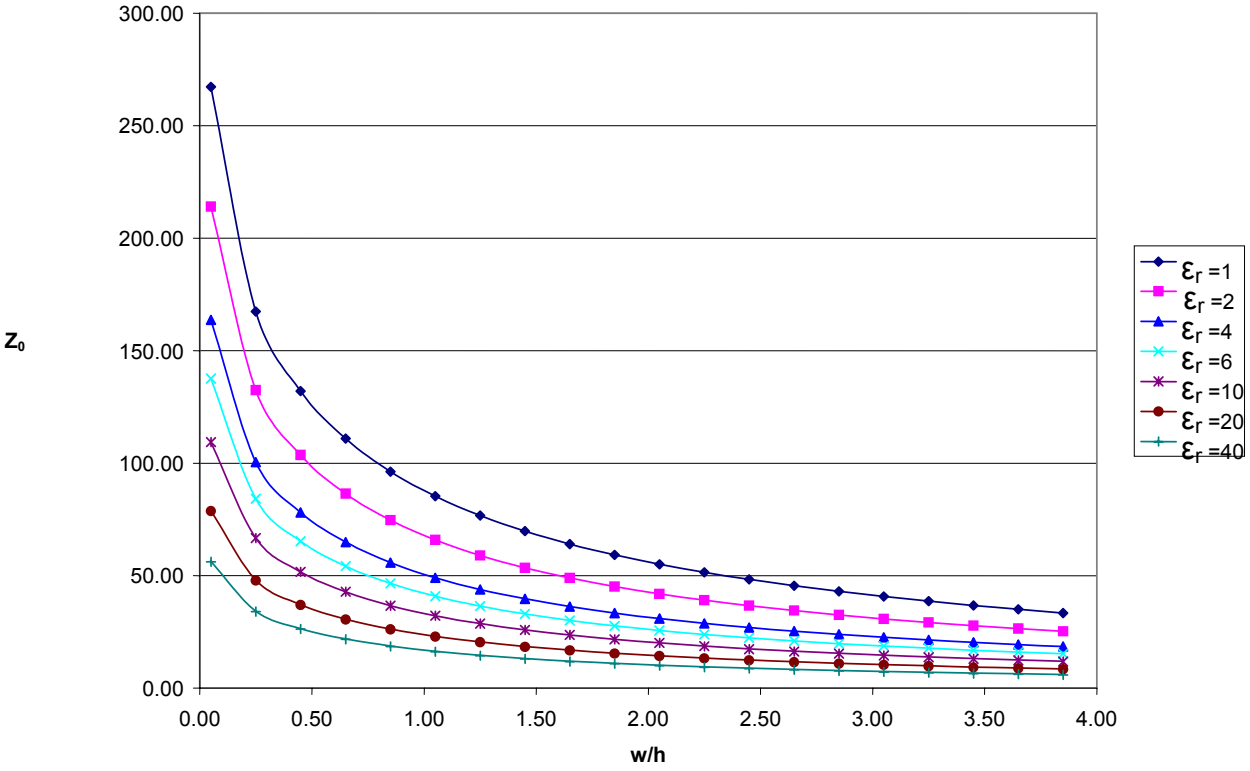

Figure 5.9: Variation of Z_0 for different dielectric constants and aspect ratio.

Figure 5.10 shows the variation of ε_{eff} with respect to aspect ratio (w/h).

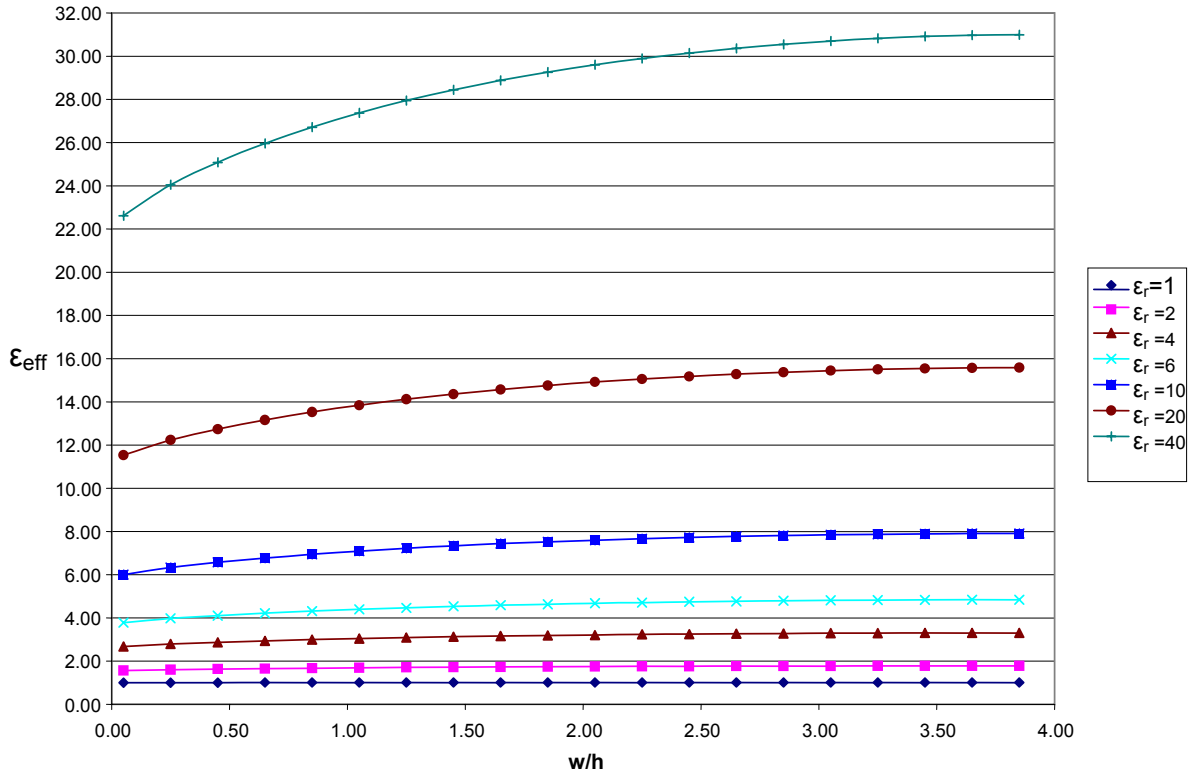

Figure 5.10: Variation of ε_{eff} for different dielectric constants and aspect ratio.

Figure 5.11 shows the variation of ε_{eff} with respect to aspect ratio (w/h). The point to note here is that q does not depend strongly on the permittivity of the substrate.

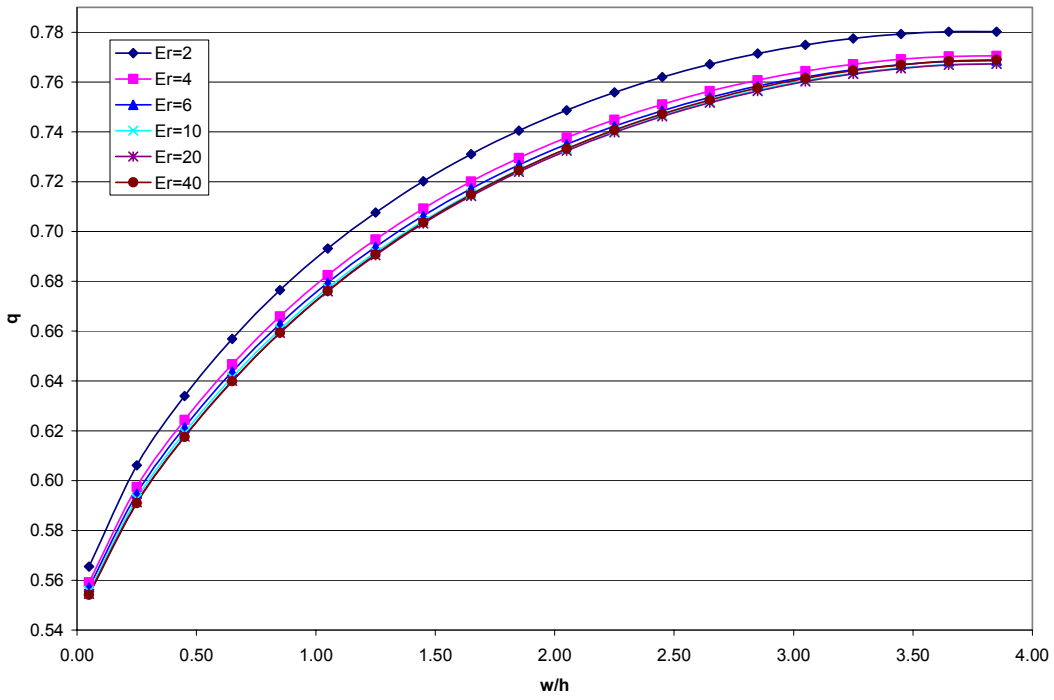

Figure 5.11: Variation of q for different dielectric constants and aspect ratio.

5.3.2 Dispersion Curves

This section discusses the comparison of the various dispersion calculation methods. First we will describe the comparison of the two dispersion calculation methods (Getsinger and Edwards and Owens) and then other dispersion methods of Yamashita, Kobayashi, and Kirschning & Jansen.

- **Getsinger's Method**

Two characteristics impedances ($Z_0 = 25\Omega \,\&\, Z_0 = 50\Omega$) were chosen as they are quite sufficient to indicate the trends in microstrip circuit design. $Z_0 = 25\Omega$ was chosen because, at lower impedances, dispersion is greater; and $Z_0 = 50\Omega$ was chosen because, it is a commonly used value.

Results for Z_0 =25 Ω

An alumina type substrate with relative permittivity ε_r = 9.9 and height (h) as 0.65 mm was considered. Now from the synthesis formula Equation (3.12) and (3.13) we get the approximate value for the width of the microstrip line ($w = 2mm$). A microstrip geometry is drawn in Sonnet Lite® with known height (h), width (w) and relative permittivity of alumina substrate (ε_r). The simulation results obtained from Sonnet Lite are as shown in Table 5.5. Now these results are compared with the theoretical values obtained by putting various variable values in Getsinger's expression Equation (3.26).

Using Equations (3.27) and (3.28) we get $f_p = 15.3$ and $G = 0.825$.

Using Equation (3.20) for obtaining the DC value of effective permittivity we get $\varepsilon_{eff} = 7.4223$. Thus theoretical values of $\varepsilon_{eff}(f)$ for various values of frequency are also shown in Table 5.5.

Table 5.5: Getsinger's Simulated and Theoretical results for Z_0 =25 Ω.

Frequency(f)	$\varepsilon_{eff}(f)$ Simulation results obtained using Sonnet Lite	$\varepsilon_{eff}(f)$ Theoretical Results obtained using Getsinger's expression
0.1	7.35603813	7.422387
1.1	7.36941226	7.432821
2.1	7.40467794	7.460219
3.1	7.46008413	7.503467
4.1	7.53288078	7.560877
5.1	7.61926752	7.630351
6.1	7.70451533	7.709552
7.1	7.79325918	7.796081
8.1	7.87400000	7.887619
9.1	7.95992672	7.982047
10.1	8.03123143	8.077508
11.1	8.11006024	8.172449
12.1	8.17532284	8.265623
13.1	8.23944416	8.356072
14.1	8.29200000	8.443098
15.1	8.34959920	8.526226
16.1	8.39600000	8.605168
17.1	8.44060624	8.679781
18.1	8.49963209	8.743206

Results for Z_0 =50 Ω

Similarly for Z_0 =50 Ω, again from the synthesis formula Equation (3.12) and (3.13) we get the approximate value for width of the microstrip line ($w = 0.7mm$). A microstrip geometry is drawn in Sonnet Lite® with this known height (h), width (w) and relative permittivity of alumina substrate (ε_r). The simulation results obtained from Sonnet Lite® are as shown in Table 5.6. Now these results are compared with the theoretical values obtained by putting various variable values in Getsinger's expression Equation (3.26).

Using Equations (3.27) and (3.28) we get $f_p = 30.6$ and $G = 1.05$.

Using Equation (3.20) to obtain the DC value of effective permittivity we get ε_{eff} =6.62368. Thus theoretical values of ε_{eff} for various values of frequency are also shown in Table 5.6.

Table 5.6: Getsinger's Simulated and Theoretical results for Z_0 =50 Ω.

Frequency(f)	$\varepsilon_{eff}(f)$ Simulation results obtained using Sonnet Lite	$\varepsilon_{eff}(f)$ Theoretical Results obtained using Getsinger's expression
0.1	6.58266349	6.623717
1.1	6.58853556	6.628119
2.1	6.60424184	6.639802
3.1	6.62951155	6.65861
4.1	6.66396497	6.684296
5.1	6.70705949	6.716531
6.1	6.75807437	6.754912
7.1	6.81609867	6.798975
8.1	6.88002379	6.848208
9.1	6.94852455	6.902068
10.1	7.02009515	6.959989
11.1	7.0930913	7.021397
12.1	7.16583408	7.085724
13.1	7.23665102	7.152417
14.1	7.30426655	7.220944
15.1	7.37022284	7.290805
16.1	7.41400000	7.361533
17.1	7.46046071	7.432702
18.1	7.4982487	7.503926

- **Edwards and Owens Method**

Results for Z_0 =25 Ω

Using the Equation (3.29) we get variation for ε_{eff} for various values of frequency. These results are summarized in Table 5.7. The value of effective permittivity at DC is same as used above for Getsinger's expression (ε_{eff} =7.4223).

We already have the simulation results with us, but adding them to the Table 5.7 for comparison.

Table 5.7: Edwards and Owens Simulated and Theoretical results for Z_0 =25 Ω.

Frequency(f)	$\varepsilon_{eff}(f)$ Simulation results obtained using Sonnet Lite	$\varepsilon_{eff}(f)$ Theoretical Results obtained using the analytical expression
0.1	7.35603813	7.422383
1.1	7.36941226	7.43208
2.1	7.40467794	7.456831
3.1	7.46008413	7.494758
4.1	7.53288078	7.543688
5.1	7.61926752	7.601333
6.1	7.70451533	7.665447
7.1	7.79325918	7.733943
8.1	7.87400000	7.804968
9.1	7.95992672	7.876940
10.1	8.03123143	7.948557
11.1	8.11006024	8.018787
12.1	8.17532284	8.086838
13.1	8.23944416	8.152125
14.1	8.29200000	8.214239
15.1	8.34959920	8.272912
16.1	8.39600000	8.327985
17.1	8.44060624	8.379384
18.1	8.49963209	8.422489

Results for Z_0 =50 Ω

Similarly the results for Z_0 = 50 Ω are shown in Table 5.8

Table 5.8: Edwards and Owens Simulated and Theoretical results for Z_0 =50 Ω.

Frequency(f)	$\varepsilon_{eff}(f)$ Simulation results obtained using Sonnet Lite®	$\varepsilon_{eff}(f)$ Theoretical Results obtained using the analytical expression
0.1	6.58266349	6.623724
1.1	6.58853556	6.628835
2.1	6.60424184	6.641990
3.1	6.62951155	6.662462
4.1	6.66396497	6.689448
5.1	6.70705949	6.722101
6.1	6.75807437	6.759561
7.1	6.81609867	6.800978
8.1	6.88002379	6.845529
9.1	6.94852455	6.892439
10.1	7.02009515	6.940987
11.1	7.09309130	6.990514
12.1	7.16583408	7.040428
13.1	7.23665102	7.090203
14.1	7.30426655	7.139375
15.1	7.37022284	7.187543
16.1	7.41400000	7.234358
17.1	7.46046071	7.279524
18.1	7.49824870	7.318552

As stated previously Getsinger and Edwards and Owens expressions are good approximately up to 18 GHz, both are compared together and the excel plot shown in Figure 5.12 shows the comparison of simulated and theoretical values (obtained from formula).

The excel plot showing the comparison of both the methods with the simulation result is as shown in Figure 5.12.

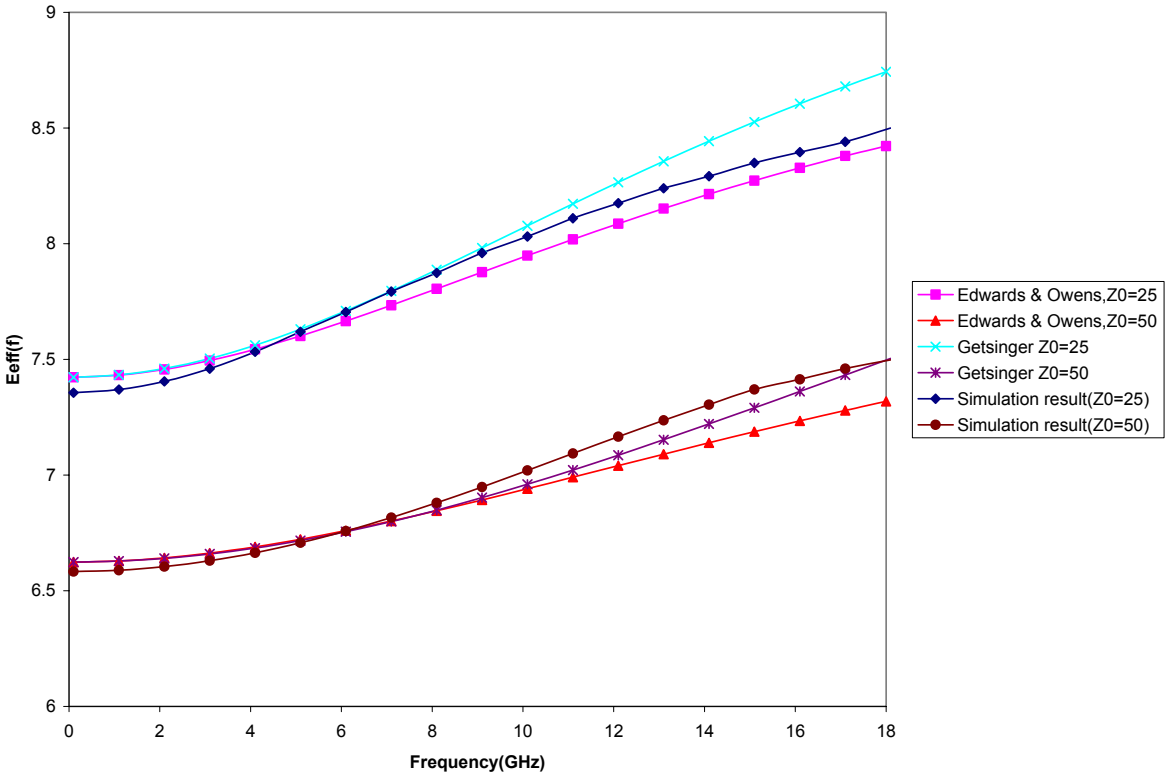

Figure 5.12: Comparison of results for Getsinger and Edwards & Owens method.

- **Yamashita, Kobayashi and Kirschning & Jansen's Methods**

For all the remaining methods for dispersion calculations, a microstrip on a GaAs substrate with $\varepsilon_r = 13$, $w = 0.254\ mm$ and $h = 0.127$ mm is considered.

Geometry with specified parameters is drawn in Sonnet Lite. The theoretical results are obtained from the Equations (3.30), (3.32) and (3.33). The value of DC effective permittivity (ε_{eff} = 9.21731) is calculated from Equation (3.23).

Table 5.9 shows the simulated and theoretical results for Yamashita's method.

Table 5.9: Simulated and theoretical results for Yamashita's method.

Frequency(f)	$\varepsilon_{eff}(f)$ Simulation results obtained from Sonnet Lite	$\varepsilon_{eff}(f)$ Theoretical Results obtained from the expression
0.1	9.154948	9.217420
2.1	9.158346	9.227887
4.1	9.169175	9.246028
6.1	9.186318	9.269108
8.1	9.208822	9.296002
10.1	9.235512	9.325999
12.1	9.265111	9.358579
14.1	9.296392	9.393332
16.1	9.328298	9.429920
18.1	9.360054	9.468058
20.1	9.391474	9.507495
22.1	9.422003	9.548015
24.1	9.452388	9.589425
26.1	9.483047	9.631553
28.1	9.514630	9.674246
30.1	9.548074	9.717367
32.1	9.582011	9.760792
34.1	9.619537	9.804411
36.1	9.656651	9.848125
38.1	9.699413	9.891844
40	9.740394	9.933309

Table 5.10 shows the simulated and theoretical results for Kobayashi's method.

Table 5.10: Simulated and theoretical results for Kobayashi's method.

Frequency(f)	$\varepsilon_{eff}(f)$ Simulation results obtained from Sonnet Lite	$\varepsilon_{eff}(f)$ Theoretical Results obtained from the expression
0.1	9.154948	9.217436
2.1	9.158346	9.227254
4.1	9.169175	9.243206
6.1	9.186318	9.262902
8.1	9.208822	9.285423
10.1	9.235512	9.310215
12.1	9.265111	9.336884
14.1	9.296392	9.365131
16.1	9.328298	9.394715
18.1	9.360054	9.425434
20.1	9.391474	9.457117
22.1	9.422003	9.489616
24.1	9.452388	9.522800
26.1	9.483047	9.556555
28.1	9.514630	9.590777
30.1	9.548074	9.625376
32.1	9.582011	9.660269
34.1	9.619537	9.695381
36.1	9.656651	9.730646
38.1	9.699413	9.766003
40	9.740394	9.799628

Table 5.11 shows the simulated and theoretical results for Kirschning and Jansen's method.

Table 5.11: Simulated and theoretical results for Kirschning and Jansen's method.

Frequency(f)	$\varepsilon_{eff}(f)$ Simulation results obtained from Sonnet Lite	$\varepsilon_{eff}(f)$ Theoretical Results obtained from the expression
0.1	9.154948	9.154955
2.1	9.158346	9.159089
4.1	9.169175	9.171188
6.1	9.186318	9.189877
8.1	9.208822	9.214092
10.1	9.235512	9.242592
12.1	9.265111	9.274060
14.1	9.296392	9.307243
16.1	9.328298	9.341071
18.1	9.360054	9.374761
20.1	9.391474	9.408121
22.1	9.422003	9.440596
24.1	9.452388	9.472929
26.1	9.483047	9.505534
28.1	9.514630	9.539054
30.1	9.548074	9.574420
32.1	9.582011	9.610000
34.1	9.619537	9.649670
36.1	9.656651	9.688652
38.1	9.699413	9.733215
40	9.740394	9.775886

The plot showing the comparison of all the three methods with the simulation result is shown in Figure 5.13.

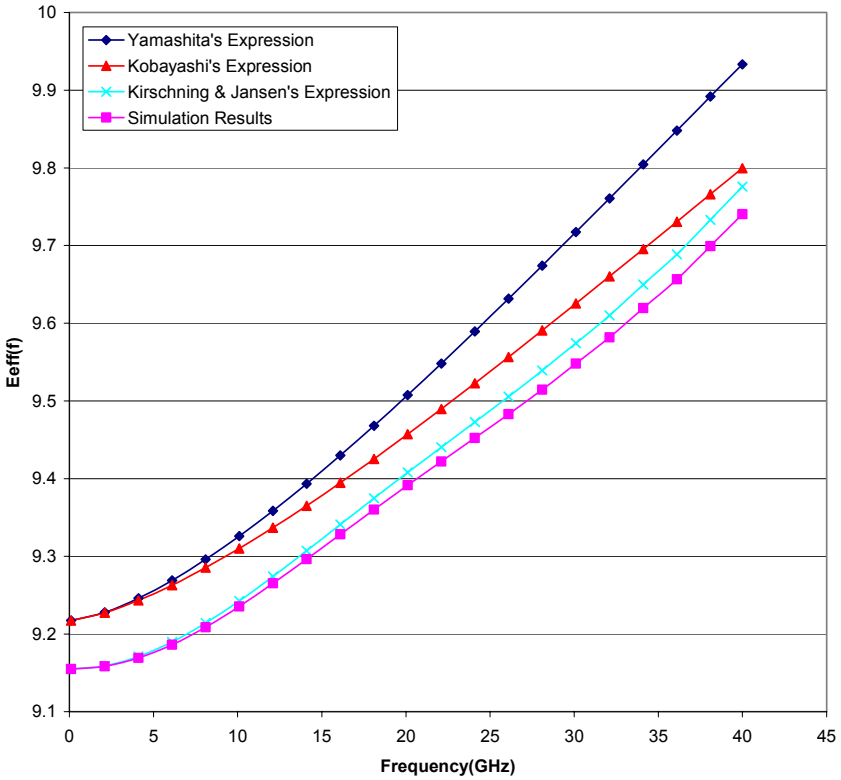

Figure 5.13: Comparison of dispersion methods with simulated results.

5.3.3 Measure of Error

The error measure $R^2{}_E\,[5]$ is given by

$$R^2{}_E = \sum_{j=1}^{j=21}\left[\frac{\varepsilon_{eff}(f)calculated - \varepsilon_{eff}(f)simulated}{\varepsilon_{eff}(f)simulated}\right]^2 j$$

was calculated and summed over all 21 data (frequency) points for each of the closed form expressions. The results of these calculations are shown in Table 5.12 and 5.13. The table also shows the r.m.s error per measurement, $\sqrt{R^2{}_E/21}$ in percent.

Table 5.12: Measure of Error and R.M.S error for Getsinger and Edwards and Owens.

Z_0	Error	Getsinger	Edwards & Owens
25	$R^2{}_E$	0.003711761	0.001336657
	RMS Error (%)	1.329476	0.797812
50	$R^2{}_E$	0.000953843	0.004174126
	RMS Error (%)	0.673951743	1.409850718

Table 5.13: Measure of Error and R.M.S. Error for various dispersion methods.

Eeff(f)	$R^2{}_E$	RMS Errors
Yamashita	0.004182856	1.411324218%
Kobayashi	0.001187833	0.752087
Kirsching & Jansen	8.90773E-05	0.205956

5.4 Summary

This chapter includes all the simulations and results obtained from Sonnelite®. Comparison of analytical and simulation results are done. Measure of error shows how close the simulated results are to the analytical results.

Chapter 6

Conclusion

In the era of high speed digital and mixed signal circuit design structure with a definite current return path (transmission line structure) are assuming more and more importance. Microstrip due to its various design advantages is particularly very attractive. The design curves for the microstrip design are very important and provide a designer with an intuitive feel for the various design parameters for microstrip lines. These curves can be used to quickly design any microstrip circuits. At high frequency microstrip design, dispersion has to be taken into account. Various closed form synthesis formulas for microstrip dispersion are developed by various researchers, which can be useful in efficient and fast CAD algorithms. Each formula has its own range of validity. Analytical results for these dispersion formulas are compared with the simulation results obtained from Sonnetlite®.

The results obtained from simulations are in close agreement to the results obtained from analytical formulas. The results obtained are only for one particular w/h ratio and relative permittivity(ε_r). The same results can be tested for different w/h ratio and relative permittivity(ε_r).

Bibliography

[1] Getsinger, W. J., “Microstrip Dispersion Model,” *IEEE Trans*., Vol. MTT–21, 1973, pp. 34–39.

[2] Yamashita, E., K Atsuki, and T. Udeda, “An approximate dispersion formula of Microstrip lines for Computer–Aided design of microwave integrated circuits,” *IEEE Trans*., Vol. MTT–27, December 1979, pp. 1036–1038.

[3] Kobayashi, M., “A dispersion formula satisfying recent requirements in Microstrip CAD,” *IEEE Trans*., Vol. MTT–36, August 1988, pp. 1246–1250.

[4] Yamashita, E., K Atsuki, and T. Hirahata, “Microstrip dispersion in wide frequency range,” *IEEE Trans*., Vol. MTT–29, June 1981, pp. 610–611.

[5] Atwater, H. A., “Tests of Microstrip dispersion formulas,” *IEEE Trans*., Vol. MTT–36, March 1988, pp. 619 –621.

[6] Schneider, M. V., “Microstrip Dispersion,” *Proc. IEEE,* Vol. 60, 1972, pp. 144–146.

[7] Kirschning, M., and R. H. Jansen, “Accurate model for effective dielectric constant of microstrip and validity up to millimeter-wave frequencies,” *Electron, Lett.,* Vol. 18, March 18, 1982, pp. 272–273.

[8] M. Kobayashi and F. Ando, “Dispersion characteristics of open microstrip lines,” *IEEE Trans. Microwave Theory Technique*, Vol. MTT–35, Feb 1987, pp. 101–105.

[9] R. A. York and R. C. Compton, “Experimental evaluation of existing CAD models for microstrip dispersion.” *Microwave Theory and Techniques, IEEE Transactions,* Vol. MTT–38, Mar 1990, pp. 327–328

[10] Silvester, P.O and Chamlian, S.V, “TEM modes in parallel line transmission structures “*Electromagnetic Compatibility, IEEE Transactions* Vol. 37, Aug 1995, pp 384 –391.

[11] T. C. Edwards, M. B. Steer, *Foundations of Interconnect and Microstrip Design,* John Wiley & Sons, Ltd.

[12] K. C. Gupta, Ramesh Garg, Inder Bahl, Prakash Bhartia, *Microstrip Lines and Slotlines,* Artech House Microwave Library.

[13] Fred Gardiol, *Microstrip Circuits*, John Wiley & Sons, INC.

[14] David H. Schrader, *Microstrip circuit analysis,* Prentice Hall PTR.

[15] Brian Young, *Digital Signal Integrity: Modeling and Simulation with Interconnects and Packages,* Prentice Hall Modern Semiconductor Design series.

[16] White papers by Cadence Design Systems.

[17] T. C. Edwards and R. P. Owens, “2–18 GHz dispersion measurements on 10–100 Ω microstrip lines on sapphire,” *IEEE Trans. Microwave Theory Tech.,* MTT–Vol. 24, Aug. 1976, pp. 506–513.

[18] Sonnet User’s Guide.